



# Induction of Nrf2-EpRE-mediated gene expression by hydroxyanthraquinones present in extracts from traditional Chinese medicine and herbs

Qihui Ren<sup>\*</sup>, Wouter Bakker, Laura de Haan, Ivonne M.C.M. Rietjens, Hans Bouwmeester

Division of Toxicology, Wageningen University and Research, Stippeneng 4, 6708 WE, Wageningen, the Netherlands

## ARTICLE INFO

Handling Editor: Dr. Bryan Delaney

### Keywords:

Herbal granules  
Traditional Chinese medicine  
Hydroxyanthraquinones  
LC-MS/MS  
Nrf2-EpRE

## ABSTRACT

Hydroxyanthraquinones that can be present in traditional Chinese medicine (TCM) and herbal extracts have claimed beneficial intestinal effects. We examined the ability of a panel hydroxyanthraquinones, and methanolic extracts from selected TCM and herbal granules to activate Nrf2-EpRE mediated gene expression using a reporter-gene assay. The results indicate that purpurin, aloë-emodin, 2-hydroxy-3-methylanthraquinone and rhein induced Nrf2 mediated gene expressions with a high induction factor (IFs > 10), with BMCL<sub>10</sub> values (the lower confidence limit of the concentration giving 10% added response above background) of 16 μM, 1.1 μM, 23 μM and 2.3 μM, respectively, while aurantio-obtusin, obtusifolin, rubiadin 1-methyl ether and emodin were less potent (IFs < 5), with BMCL<sub>10</sub> values for added response above background level of 4.6 μM, 15 μM, 9.8 μM and 3.8 μM, respectively. All TCM extracts and the herbal extracts of *Aloe Vera*, *Polygonum multiflorum*, *Rubia cordifolia* and *Rheum officinale* activated the Nrf2-EpRE pathway. Of the TCM extracts, Chuan-Xin-Lian-Kang-Yan-Pian was the most potent Nrf2-inducer. LC-MS/MS analysis indicated the presence of selected hydroxyanthraquinones in the extracts and herbs, in part explaining their Nrf2-EpRE mediated activity. In conclusion, different hydroxyanthraquinones have different potencies of Nrf2 activation. The Nrf2 activation by extracts from TCM and herbs can be partially explained by the presence of selected hydroxyanthraquinones.

## 1. Introduction

Traditional Chinese medicine (TCM) continues to receive attention as potentially effective alternative treatment of several human complaints including intestinal problems (Teschke et al., 2015; Zhang et al., 2020). Hydroxyanthraquinones are the main bioactive ingredients naturally present in TCM used against intestinal complaints and represent a group of chemicals that share a 9,10-anthraquinone backbone (Fig. 1A) with hydroxyl substituents at different positions (Fig. 1B). Hydroxyanthraquinones have been found to be abundantly present in many plant families, such as, Polygonaceae (Gao et al., 2017; Hsu and Chung, 2012; Sharifi-Rad et al., 2022), Rubiaceae (Tessier et al., 1981;

Wang et al., 2013, 2020) and Liliaceae (Zahn et al., 2008). Specific herbs from these plant families like *Rheum officinale*, *Rheum palmatum*, *Cassia obtusifolia*, *Cassia tora*, *Aloe ferox*, *Aloe vera*, *Polygonum multiflorum*, and *Rubia cordifolia* are used in TCM preparations prescribed to treat intestinal complaints (Akbar, 2020; Ali et al., 2021; Fan et al., 2018; Gong et al., 2017; Gu et al., 2020; Rahman et al., 2021; Rejiya et al., 2009). Because of an increased use and thus increased consumer exposure to botanical products containing hydroxyanthraquinones and their derivatives, the European Food Safety Authority (EFSA) raised concerns over the safety of use of these products as food supplements (EFSA Panel on Food Additives and Nutrient Sources added to Food (ANS), 2018). In its 2018 opinion on hydroxyanthracenes EFSA concluded that

**Abbreviations:** BMD, benchmark dose; BMCL<sub>10</sub>, lower bound of the benchmark concentration causing 10% added effect above background level; CALUX, Chemical Activated Luciferase gene eXpression; EFSA, European Food Safety Authority; EpRE, electrophile responsive element; GST, glutathione S-transferases; HO-1, heme oxygenase-1; IF, induction factor; Keap1, Kelch-like erythroid-cell-derived protein with CNC homology-associated protein 1; NQO1, NAD(P)H:quinone oxidoreductase1; Nrf2, nuclear factor erythroid 2-related factor 2; RLU, relative light unit; TCM, traditional Chinese medicine; TNF-α, tumor necrosis factor alpha; BZP, Ba Zheng Pian; CXLKYP, Chuan Xin Lian Kang Yan Pian; JWFFTSP, Jia Wei Fang Feng Tong Sheng Pian; JDGCP, Jiang Dan Gu Chun Pian; KZP, Kang Zhong Pian; SZJZP, Shan Zha Jiang Zhi Pian; TCP, Tong Chang Pian; ZGSJTP, Zuo Gu Shen Jing Tong Pian.

<sup>\*</sup> Corresponding author.

E-mail address: [qihui.ren@wur.nl](mailto:qihui.ren@wur.nl) (Q. Ren).

<https://doi.org/10.1016/j.fct.2023.113802>

Received 15 December 2022; Received in revised form 17 April 2023; Accepted 25 April 2023

Available online 26 April 2023

0278-6915/© 2023 The Authors. Published by Elsevier Ltd. This is an open access article under the CC BY-NC-ND license (<http://creativecommons.org/licenses/by-nc-nd/4.0/>).

hydroxyanthracenes and related hydroxyanthracenes derivatives including some of hydroxyanthraquinones like rhein, aloe-emodin and emodin should be regarded as being genotoxic and carcinogenic unless there are particular data to the contrary, such as for the hydroxyanthraquinone rhein (EFSA Panel on Food Additives and Nutrient Sources added to Food (ANS), 2018). In addition to their use against intestinal complaints (mainly as a laxative), hydroxyanthraquinones have been reported to cover a broad spectrum of other activities, including anti-cancer, antiarthritic, anti-bacterial, antifungal, anti-inflammatory and antioxidative effects (Antonisamy et al., 2019; Hou et al., 2018; Hu et al., 2021; Li and Jiang, 2018). So far only the biological activities of rhein, emodin and aloe-emodin have been relatively well studied, and much needs to be revealed for other hydroxyanthraquinones.

The mode of action underlying the biological effects of hydroxyanthraquinones may in part be related to the activation of the Nrf2 pathway. Nrf2 (nuclear factor erythroid 2-related factor 2) is the major regulator of electrophile responsive element (EpRE)-mediated gene expression (de Oliveira et al., 2021; Paudel et al., 2018). Under homeostatic conditions Nrf2 is kept in the cytoplasm by Keap1 (Kelch-like erythroid-cell-derived protein with CNC homology-associating protein 1). When oxidative or electrophilic compounds attack multiple cysteine residues on Keap1, Nrf2 can be released from Keap1 and subsequently translocate to the nucleus. Upon associating with other transcription factors, Nrf2 binds to the EpRE and activates EpRE-mediated gene expression (Deshmukh et al., 2017). The downstream effects of Nrf2 induction have been described in many studies using omics approaches including both transcriptomics (Otsuki et al., 2021; Quiles et al., 2017; Shelton et al., 2015) as well as proteomics (Liu et al., 2022; Shelton et al., 2015). Around 250 genes are known to be regulated by the Nrf2-EpRE pathway, which are related to cell homeostasis, anti-oxidation, detoxification and drug delivery (Ahuja et al., 2022; Baba et al., 2022; Ding et al., 2022). Well known target genes include heme oxygenase-1 (HO-1), NAD(P)H:quinone oxidoreductase1 (NQO1), glutathione S-transferases (GST) (Liu et al., 2022; Muzolf-Panek et al., 2008; Papadi et al., 2019). In addition, the Nrf2-EpRE activation is critical for regulating the balance of cytokines, including interleukins, interferons, tumor necrosis factor- $\alpha$  (TNF- $\alpha$ ) (Ahmed et al., 2017).

Results from several *in vivo* rodent studies showed Nrf2 induction related effects following oral administration of individual hydroxyanthraquinones. Upon oral administration, rhein was reported to induce anti-inflammatory effects in intestine and liver by activation of Nrf2 (Antonisamy et al., 2019; Bu et al., 2018; Zhuang et al., 2019a). In more detail, in these studies rhein increased the level of nuclear Nrf2 in a dose dependent manner and induced related enzyme expression like expression of heme oxygenase-1, and of glutathione peroxidase while rhein decreased serum, ileum and liver levels of interleukin-6, interleukin-1 $\beta$  and TNF- $\alpha$  (Antonisamy et al., 2019; Bu et al., 2018; Zhuang et al., 2019a). Emodin orally administered to rodents was also reported to increase the expression level of nuclear Nrf2 and heme oxygenase-1 in the intestine, brains and pulmonary tissues of these rats (Li et al., 2020; Shang et al., 2021; Shen et al., 2022; Tian et al., 2018). Via Nrf2

activation emodin also attenuated pulmonary fibrosis and hepatotoxicity (Li et al., 2020; Shang et al., 2021; Shen et al., 2022; Tian et al., 2018). No *in vivo* Nrf-2 related data could be found on other hydroxyanthraquinones.

The aim of present study was to quantify the Nrf2-activation potency of a panel of hydroxyanthraquinones and extracts of TCM or single herb-based granules containing hydroxyanthraquinones, and elucidate to what extent the hydroxyanthraquinones are responsible for the Nrf2-EpRE mediated gene expression by the extracts. To this end, a high-throughput method, the Nrf2-U2OS-based CALUX reporter gene assay, was used to quantify the potencies for Nrf2 activation of 16 hydroxyanthraquinones and methanolic extracts of 8 TCM and 8 single herb-based granules. In addition, the HO-1 gene expression by selected hydroxyanthraquinones was quantified by RT-qPCR to validate the reporter gene results. Lastly, concentration of our selected hydroxyanthraquinones in extracts of TCM and single herb-based granules was determined by liquid chromatography with tandem mass spectrometry (LC-MS/MS) analysis. Nrf2 activation by a large series of hydroxyanthraquinones has not been reported before and this also holds for the hydroxyanthraquinones containing extracts. It revealed that especially purpurin, with 3 hydroxyl moieties on one of its aromatic rings, showed a high potential for Nrf2 activation. Given that these hydroxyl substituents are electron donating groups this may point at a mode of action related to ionization and ROS formation rather than to electrophilicity as the mode of action underlying the Nrf2 induction, a novel finding that is of interest for future investigations.

## 2. Materials and methods

### 2.1. Chemicals, botanicals, traditional Chinese medicines (TCM) and reagents

The hydroxyanthraquinones selected for this study (Table 1, Chemical structures were drawn using ChemDraw 18.0 (PerkinElmer, Waltham, USA)) were obtained from Sigma Aldrich (Zwijndrecht, The Netherlands) and Wuhan ChemFaces Biochemical Co., Ltd. (Wuhan, China). Single herb-based granules were purchased from De Natuur-Apotheek BV (Pijnacker, The Netherlands) (Table 2). TCM were purchased from Activeherbs (website [activeherbs.com](http://activeherbs.com), USA) (Table 3).

Methanol of analytical grade was obtained from Fisher Scientific (Loughborough, United Kingdom), curcumin, formic acid and acetonitrile were ordered from Sigma Aldrich (Zwijndrecht, The Netherlands), dimethyl sulfoxide (DMSO) was purchased from Acros Organics (Geel, Belgium). Dulbecco's Modified Eagle Medium with Ham's Nutrient Mixture F-12 (1:1) (DMEM/F12), DMEM/F12 without phenol red, trypsin 0.05% EDTA, nonessential amino acids (NEAA) and phosphate-buffered saline pH 7.4 (PBS), geneticin (G418), penicillin/streptomycin, were purchased from Gibco (Carlsbad, California, USA). Fetal bovine serum (FBS) was purchased from Invitrogen (Breda, The Netherlands). Dextran-coated charcoal-stripped fetal calf serum (DCC-FCS) was obtained from Thermo Scientific (Waltham, Massachusetts, USA).

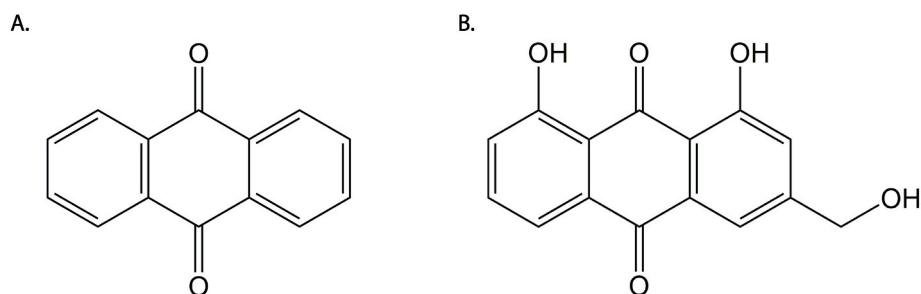
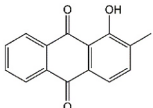
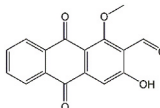
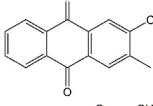
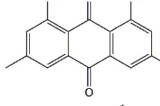
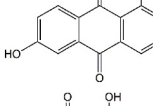
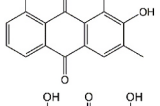
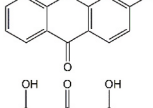
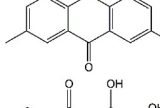
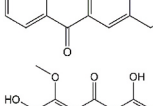
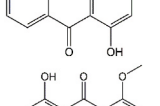
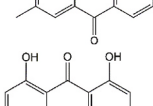
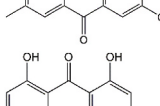
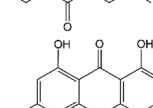
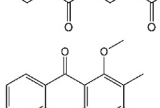
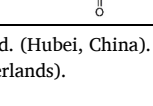
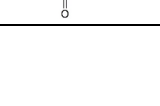


Fig. 1. Chemical structures showing the basic skeleton of 9,10-anthraquinones (A) and an example of an anthraquinone containing hydroxyl groups (rhein) as a hydroxyanthraquinone(B).

**Table 1**  
Overview of the hydroxyanthraquinones studied and their chemical structures.

Name (CAS No.)	Structure	Name (CAS No.)	Structure
1 1-Hydroxy-2-methylantraquinone (6268-09-3) <sup>a</sup>		9 Damnacanthal (477-84-9) <sup>b</sup>	
2 2-Hydroxy-3-methylantraquinone (17241-40-6) <sup>a</sup>		10 Emodin (518-82-1) <sup>b</sup>	
3 6-Hydroxyrubiadin (87686-86-0) <sup>a</sup>		11 Obtusifolin (477-85-0) <sup>a</sup>	
4 Alizarin (72-48-0) <sup>b</sup>		12 Physcion (521-61-9) <sup>b</sup>	
5 Aloe-emodin (481-72-1) <sup>b</sup>		13 Purpurin (81-54-9) <sup>b</sup>	
6 Aurantio-obtusin (67979-25-3) <sup>b</sup>		14 Questin (3774-64-9) <sup>a</sup>	
7 Chrysophanol (481-74-3) <sup>b</sup>		15 Rhein (478-43-3) <sup>b</sup>	
8 Citreosein (481-73-2) <sup>a</sup>		16 Rubiadin 1-methyl ether (7460-43-7) <sup>a</sup>	

<sup>a</sup>, obtained from Wuhan ChemFaces Biochemical Co., Ltd. (Hubei, China).

<sup>b</sup>, obtained from Sigma Aldrich (Zwijndrecht, The Netherlands).

## 2.2. Methanol extraction of single herb-based granules and TCMs

First, 0.2 g of single herb-based granules or TCMs in powder form was soaked in 20 ml of 70% (v/v) methanol at room temperature for 30 min and subjected to ultrasonication (40 kHz, 500 W) at room temperature for 30 min (Wei et al., 2013). The extract was centrifuged at 5000 rpm (3717g, 2-16 KL, Sigma, Germany) for 20 min, the supernatant was filtered through filter paper (MN 615 ¼, Ø 240 mm, Machery & Nagel, Düren, Germany) and evaporated to dryness under a nitrogen flow (Soib et al., 2020). The resulting residues were stored at -20 °C until further use (i.e. for analysis by the Nrf2 CALUX and Cytotox CALUX assays and LC-MS/MS analysis) (Soib et al., 2020).

## 2.3. Cell culture

Both the Nrf2 CALUX cells and the Cytotox CALUX cells (BDS, Amsterdam, the Netherlands) are based on human osteoblastic osteosarcoma U2OS cells (van der Linden et al., 2014). The Nrf2 CALUX cells contain the firefly luciferase gene under control of four Electrophile Responsive Elements (EpRE) while the Cytotox CALUX cells are modified to constantly express luciferase through transfection with a vector carrying a luciferase reporter gene (van der Linden et al., 2014). The cells were maintained in a humidified atmosphere with 5% CO<sub>2</sub> at 37 °C and cultured in DMEM/F12 supplemented with 7.5% (v/v) FBS, 1% (v/v) NEAA, penicillin/streptomycin (final concentrations 10 U/ml and 10 µg/ml, respectively) and 0.2 mg/ml G418 (added once a week).

Every 2 or 3 days, the cells were sub-cultured.

## 2.4. Nrf2 CALUX reporter gene assay

The potential induction of Nrf2-EpRE mediated gene expression by individual compounds and extracts of TCM powders and of single herb-based granules was tested by measuring the induction of luciferase activity in the Nrf2 CALUX cells. Firstly, Nrf2 CALUX cells were seeded in the 60 inner wells of 96-well white plates at a density of  $3 \times 10^4$  cells/well in 100 µl culture medium. The outer wells were filled with 200 µl PBS. The plates were incubated for 24 h until the cells formed confluent monolayers. Subsequently, the medium was replaced by assay medium containing solvent control (DMSO, 1% v/v or 2% v/v), pure compounds or extracts of single herb-based granules/TCMs, respectively. And the cells were exposed to the sample of interest for 24 h. Curcumin was used as the positive control.

After the 24-h exposure, medium was removed and cells were washed with 100 µl 0.5 × PBS, followed by the addition of 30 µl low salt lysis buffer (containing 10 mM Tris, 2 mM DTT and 2 mM trans-1,2-diaminocyclohexane-N,N,N',N'-tetra-acetic acid mono-hydrate (CDTA), pH 7.8) to each well. For the swelling and lysis of the cells the plates were placed on ice for 15 min and then overnight at -80 °C. In order to determine the luciferase activity in the lysates, 100 µl of Flash mix (20 mM tricine, 1.07 mM (MgCO<sub>3</sub>)<sub>4</sub> Mg(OH)<sub>2</sub>·5H<sub>2</sub>O, 2.67 mM MgSO<sub>4</sub>, 0.1 mM EDTA·2H<sub>2</sub>O, 2 mM DTT, 0.47 mM D-luciferin, 5 mM ATP, the pH of the mix was 7.8) was added in every well. Luciferase activity was

**Table 2**

List of single herb-based granules, their botanical origin and hydroxyanthraquinones which are reported to be present in these products.

Product name	Botanical origin	Described tentative presence of hydroxyanthraquinones in plant species	References
Aloe	<i>Aloe Vera</i> , Herba	Aloe-emodin	Rahman et al. (2021)
Cassia Seed	<i>Cassia obtusifolia/tora</i> , Semen	Aloe-emodin, aurantio-obtusin, emodin, chrysophanol, obtusifolin, physcion, questin, rhein	(Ali et al., 2021; Choi et al., 2019; Guo et al., 2017; Hou et al., 2018; Paudel et al., 2018; Zhang et al., 2012)
Madder	<i>Rubia (cordifolia)</i> , Radix	1-Hydroxy-2-methylanthraquinone, 6-hydroxyrubiadin, alizarin, emodin, purpurin	(Balachandran et al., 2021; Singh et al., 2021) Miyazawa and Kawata, 2006; Shen et al., 2018; Singh et al., 2021)
Morinda	<i>Morinda officinalis</i> , Radix	1-Hydroxy-2-methylanthraquinone, aloe-emodin, emodin, rubiadin-1-methyl ether	(Anh et al., 2021; M. Wang et al., 2019)
Oldenlandia	<i>Hedyotis diffusa</i> , Herba	2-Hydroxy-3-methylanthraquinone	(Wang et al., 2013; Yang et al., 2017)
Polygonum (Ho Shou Wu)	<i>Polygonum multiflorum</i>	Aloe-emodin, chrysophanol, emodin, physcion, rhein	Yuan et al. (2020)
Rhubarb	<i>Rheum officinale</i> , Rhizoma	Aloe-emodin, chrysophanol, emodin, physcion, rhein	(Alehaideb et al., 2019; Chen et al., 2020; Su et al., 2020)
Senna Leaf	<i>Cassia senna</i> , Folium	Aloe-emodin, rhein	Meier et al. (2017)

measured in relative light units (RLU) using a GloMax-Multi + Microplate Mutimode Reader (Promega, Sunnyvale, California, USA).

The results are presented as the Induction Factor (IF), which is the measured RLU value divided by the mean RLU value of the solvent control. For curcumin, used as the positive control, the minimal IF was set to be 8. Samples presenting an induction of 2.0-fold or higher were considered as inducers of Nrf2-EpRE mediated-gene expression (van der Linden et al., 2014). The potency of Nrf2 activation was also assessed by determining the BMCL<sub>10</sub> which is the lower 95% confidence limit of the concentration inducing 10% added response above background. Using added instead of extra response one can calculate a BMCL<sub>10</sub> without the need for defining the concentration that gives a maximum 100% response. All experiments were conducted under reduced light conditions. All experiments were repeated three times unless indicated otherwise.

## 2.5. Cytotox CALUX reporter gene assay

The Cytotox CALUX cells, that express a constant level of luciferase, serve as a cytotoxicity indicator and a control for non-specific luciferase activation. The decrease in luciferase activity in the presence of cytotoxicity was utilized to ensure that non-cytotoxic concentrations were evaluated and that the extracts did not include any residual organic solvents that could cause cytotoxicity. Enhanced luciferase activity in these Cytotox CALUX cells, on the other hand might indicate the presence of compounds that stabilize the luciferase enzyme, resulting in higher luciferase activity without an increase in gene expression. The Cytotox CALUX cells were treated and exposed in the same way that the Nrf2 CALUX cells were treated and exposed. The results are also presented as the IF, which is the measured RLU value divided by the mean RLU value of the solvent control.

**Table 3**

List of traditional Chinese medicines (TCMs) and their ingredients as indicated on the label. Botanicals known to potentially contain hydroxyanthraquinones and of which extracts were also included in the present study are printed in bold.

TCMs	Ingredients on label
Ba Zheng Pian (BZP)	Fringed pink aerial part ( <i>Dianthus superbus</i> ) Asian plantain seed ( <i>Plantago asiatica</i> ) Knotweed aerial part ( <i>Polygonum aviculare</i> ) <b>Chinese rhubarb root and rhizome (<i>Rheum officinale</i>)</b> Talcum Akebia vine ( <i>Akebia trifoliata</i> ) Gardenia fruit ( <i>Gardenia jasminoides</i> ) Chinese licorice root prepared ( <i>Glycyrrhiza uralensis</i> ) Soft rush pith ( <i>Juncus effusus</i> )
Chuan Xin Lian Kang Yan Pian (CXLYKYP)	Andrographis aerial part ( <i>Andrographis paniculata</i> ) Dandelion whole plant ( <i>Taraxacum officinale</i> ) Heal-all fruit spike ( <i>Prunella vulgaris</i> ) <b>Hedyotis whole plant (<i>Hedyotis diffusa</i>)</b> Siler root ( <i>Saposhnikovia divaricata</i> ) Schizonepeta aerial part ( <i>Schizonepeta tenuifolia</i> ) Chinese mint aerial part ( <i>Mentha haplocalyx</i> ) Cassia twig ( <i>Cinnamomum cassia</i> ) <b>Aloe vera gel (<i>Aloe barbadensis</i>)</b> <b>Indian laburnum seed (<i>Cassia obtusifolia</i>)</b> Gardenia fruit ( <i>Gardenia jasminoides</i> ) Asian plantain seed ( <i>Plantago asiatica</i> ) Platycodon root ( <i>Platycodon grandiflora</i> ) Anemarrhena rhizome ( <i>Anemarrhena asphodeloides</i> ) Sichuan lovage rhizome ( <i>Ligusticum chuanxiong</i> ) Dong quai root ( <i>Angelica sinensis</i> ) Chinese peony root ( <i>Paeonia lactiflora</i> ) Barbed skullcap root ( <i>Scutellaria baicalensis</i> ) Forsythia fruit ( <i>Forsythia suspensa</i> ) Chinese licorice root ( <i>Glycyrrhiza uralensis</i> ) bai-zhu atractylodes rhizome ( <i>Atractylodes macrocephala</i> )
Jia Wei Fang Feng Tong Sheng Pian (JWFFTSP)	Chinese hawthorn fruit ( <i>Crataegus pinnatifida</i> ) <b>Fo-Ti root cured (<i>Polygonum multiflorum</i>)</b> Lycium fruit ( <i>Lycium barbarum</i> ) Polygonatum rhizome ( <i>Polygonatum sibiricum</i> ) Reishi fruiting body ( <i>Ganoderma lucidum</i> ) Asian water plantain rhizome ( <i>Alisma orientale</i> ) Turmeric rhizome ( <i>Curcuma longa</i> ) Safflower flower ( <i>Carthamus tinctorius</i> ) Dong quai root ( <i>Angelica sinensis</i> ) Sichuan lovage rhizome ( <i>Ligusticum chuanxiong</i> ) Sarcandra whole plant ( <i>Sarcandra glabra</i> ) Barbed skullcap whole plant ( <i>Scutellaria barbata</i> ) NO Common Name whole plant ( <i>Salvia chinensis</i> ) Job's tears seed ( <i>Coix lacryma-jobi</i> ) <b>Hedyotis whole plant (<i>Hedyotis diffusa</i>)</b> Herb-paris rhizome ( <i>Paris polyphylla</i> )
Jiang Dan Gu Chun Pian (JDGCP)	Chinese hawthorn fruit ( <i>Crataegus pinnatifida</i> ) Chinese salvia root ( <i>Salvia miltiorrhiza</i> ) <b>Fo-Ti root cured (<i>Polygonum multiflorum</i>)</b> <b>Chinese rhubarb root and rhizome prepared (<i>Rheum officinale</i>)</b> Pinellia rhizome cured ( <i>Pinellia ternata</i> ) Oyster shell Semiaquilegia root ( <i>Semiaquilegia adoxoides</i> ) Chinese arisaema rhizome prepared ( <i>Arisaema erubescens</i> )
Kang Zhong Pian (KZP)	Peach seed ( <i>Prunus persica</i> ) Hemp fruit ( <i>Cannabis sativa</i> ) <b>Chinese rhubarb root and rhizome (<i>Rheum officinale</i>)</b> <b>Fo-Ti root cured (<i>Polygonum multiflorum</i>)</b> Dong quai root ( <i>Angelica sinensis</i> ) Notopterygium rhizome and root ( <i>Notopterygium incisum</i> )
Shan Zha Jiang Zhi Pian (SZJZP)	
Tong Chang Pian (TCP)	

(continued on next page)



Table 3 (continued)

TCMs	Ingredients on label
Zuo Gu Shen Jing Tong Pian (ZGSJTP)	Frankincense resin ( <i>Boswellia carterii</i> ) Myrrh resin ( <i>Commiphora myrrha</i> ) Spatholobus stem ( <i>Spatholobus suberectus</i> ) Corydalis yanhusuo rhizome ( <i>Corydalis yanhusuo</i> ) <b>Morinda root (<i>Morinda officinalis</i>)</b> Siegesbeckia aerial part ( <i>Siegesbeckia orientalis</i> ) Chinese clematis root ( <i>Clematis chinensis</i> ) Turmeric rhizome ( <i>Curcuma longa</i> ) Rehmannia root cured ( <i>Rehmannia glutinosa</i> ) Sichuan lovage rhizome ( <i>Ligusticum chuansiang</i> ) Lycopodium japonicum whole plant ( <i>Lycopodium japonicum</i> )

## 2.6. Reverse transcription-quantitative polymerase chain reaction (RT-qPCR) analysis

RT-qPCR was performed to investigate the Nrf2 activation by hydroxyanthraquinones at the mRNA level. To this end, both Nrf2 CALUX cells and wild type U2OS cells were seeded in 6-well plates at a density of  $3.6 \times 10^4$  cells/well in 2.5 ml culture medium and incubated in a humidified atmosphere 5% CO<sub>2</sub> at 37 °C for 24 h to form confluent monolayers. Then cells were exposed for 24 h to purpurin (200 μM) and aloe-emodin (100 μM), their respective highest concentration used in Nrf2 CALUX reporter gene assay for 24 h. After that, mRNA was isolated by using the QIAshredder and RNeasy® mini kit (Qiagen, Venlo, The Netherlands). The quality and quantity of isolated mRNA were measured by Nanodrop (ND-1000; ThermoScientific, Waltham, MA, USA). Then the isolated mRNA was reverse-transcribed to cDNA using the QuantiTect® reverse transcription kit (Qiagen, Venlo, The Netherlands). RT-qPCR analysis was performed in accordance with the instruction of manufacturer using the RotorGene® SYBR® kit and RotorGene® 6000 cycler. Actin beta (ACTB) was used as housekeeping gene, and Heme oxygenase-1 (HO-1) was select as a downstream gene of the Nrf2-EpRE pathway (Lin et al., 2021). The primers were obtained from QuantiTect® primer assay, and included Hs\_ACTB\_1\_SG and Hs\_Hmox1\_1\_SG. Relative mRNA expression levels of the HO-1 gene were normalized by comparing to ACTB (housekeeping gene) expression levels, and calculated using the 2-ΔΔCt method (Livak and Schmittgen, 2001).

## 2.7. Liquid chromatography mass spectrometry (LC-MS/MS) analysis of extracts of single herb-based granules and TCMs

Extracts of single herb-based granules and TCMs were analysed by LC-MS/MS to identify and quantify the potential presence of the hydroxyanthraquinones that displayed a positive induction of the Nrf2-EpRE mediated gene expression. The samples were prepared as follows: the extracts of single herb-based granules and TCMs in DMSO were dissolved in methanol (final concentration of DMSO less than 1% (v/v)), and centrifuged at 10,000 rpm (9351g, centrifuge 5424, Eppendorf, Hamburg, Germany) for 10 min and the supernatant was collected. For the calibration curve, a range of concentrations of different compounds (0–20 μM) was prepared in methanol. The injection volume for subsequent LC-MS/MS analysis was 1 μl. The samples were analysed by an ultra-high-performance liquid chromatography system coupled with a tandem triple quadrupole mass spectrometer, fitted with an ESI source (Shimadzu LCMS-8045, Shimadzu, Japan). The ESI source was operated in both negative and positive mode, the fragment ions m/z were obtained. Samples were injected onto a Phenomenex Kinetex C18 column (1.7 μm, 2.1 × 50 mm; Phenomenex, Utrecht, Netherlands). The gradient applied started at 100% solvent A (0.1% (v/v) formic acid in nanopure water) and 0% solvent B (0.1% (v/v) formic acid in acetonitrile), and dropped to 50% solvent A at 3 min and 30% solvent A at 10 min. Solvent B reached 100% at 12 min and was held at 100% until 15 min, when the

gradient was modified back to the original 100% solvent A, 0% solvent B. The gradient program ended at 22 min.

Chromatographic peaks were identified by comparison of retention time and ion values with those of commercially available reference compounds of analytical grade. More details on the LC-MS/MS identification and quantification of the selected hydroxyanthraquinones are shown in Table S9.

## 2.8. Data analysis

Data from the Nrf2 CALUX assay and the Cytotox CALUX assay were processed by Graphpad Prism 5 (San Diego, USA). By dividing the mean measured RLU value of each sample by the mean RLU of the solvent control of each experimental unit, the IF was obtained (96-well plate). The data are reported as the average IF of at least three independent experiments with a standard error of the mean (SEM). For calculating the BMCL<sub>10</sub> values for 10% added response above background levels the results of the Nrf2 CALUX assay were corrected using the respective results from the Cytotox CALUX assay. The benchmark dose (BMD) method was used to analyse the in vitro corrected concentration response curves from Nrf2 CALUX assay. According to the European Food Safety Authority's manual (2020), benchmark concentration (BMC) was calculated using the BMD modelling web tool (2020) using added instead of extra risk and 10% response.

Shimadzu Lab solutions software was used to gather and process the LC-MS/MS data.

To predict the combined effects of hydroxyanthraquinones in extracts of single herb-based granules and TCM on Nrf2-EpRE mediated gene expression, the concentration of each hydroxyanthraquinone detected in the extracts was expressed in terms of aloe-emodin equivalents using a relative potency factor (RPF) (See Eq. (1) and Eq. (2))

$$C_{\text{total}} = \sum (C_i \times \text{RPF}_i) \quad (1)$$

Where  $C_{\text{total}}$  is the total concentration of hydroxyanthraquinones in extracts of single herb-based granules or TCM expressed in aloe-emodin equivalent,  $C_i$  is the concentration of hydroxyanthraquinone  $i$  in the extract experimentally detected by LC-MS/MS.  $\text{RPF}_i$  was defined using Eq. (2) based on the BMCL<sub>10</sub> of aloe-emodin (BMCL<sub>10, aloe-emodin</sub>) and the BMCL<sub>10</sub> of hydroxyanthraquinone  $i$  (BMCL<sub>10, i</sub>) in the corrected concentration response curve of Nrf2-CALUX assay, RPF of aloe-emodin was set at 1.0.

$$\text{RPF}_i = (\text{BMCL}_{10, \text{aloe-emodin}}) / (\text{BMCL}_{10, i}) \quad (2)$$

The calculated IFs of single herb-based extracts and TCM extracts were calculated based on corrected concentration response curve of the Nrf2 CALUX assay of aloe-emodin.

## 3. Results

### 3.1. Activity of hydroxyanthraquinones in induction of Nrf2 mediated gene expression

Fig. 2 shows the concentration dependent Nrf2 activation by 16 individual hydroxyanthraquinones as detected by the Nrf2 CALUX reporter gene assay. The figure also presents the results of the Cytotox CALUX reporter gene assay detecting the potential cytotoxicity and non-specific luciferase stabilization by the hydroxyanthraquinones. Curcumin was used as positive control in each plate (see Fig. S1). Fig. 2A–D shows that especially purpurin, and also aloe emodin, 2-hydroxy-3-methylanthraquinone and rhein displayed relatively high potencies for the induction of Nrf2 mediated gene expression. The IFs obtained with these compounds in the Nrf2 CALUX assay ranged from 10.1 to 44.5 at the highest concentration tested at which maximum Nrf2 induction was not yet achieved. For aloe-emodin and rhein there was no response in the Cytotox CALUX assay at any of the concentrations tested, also

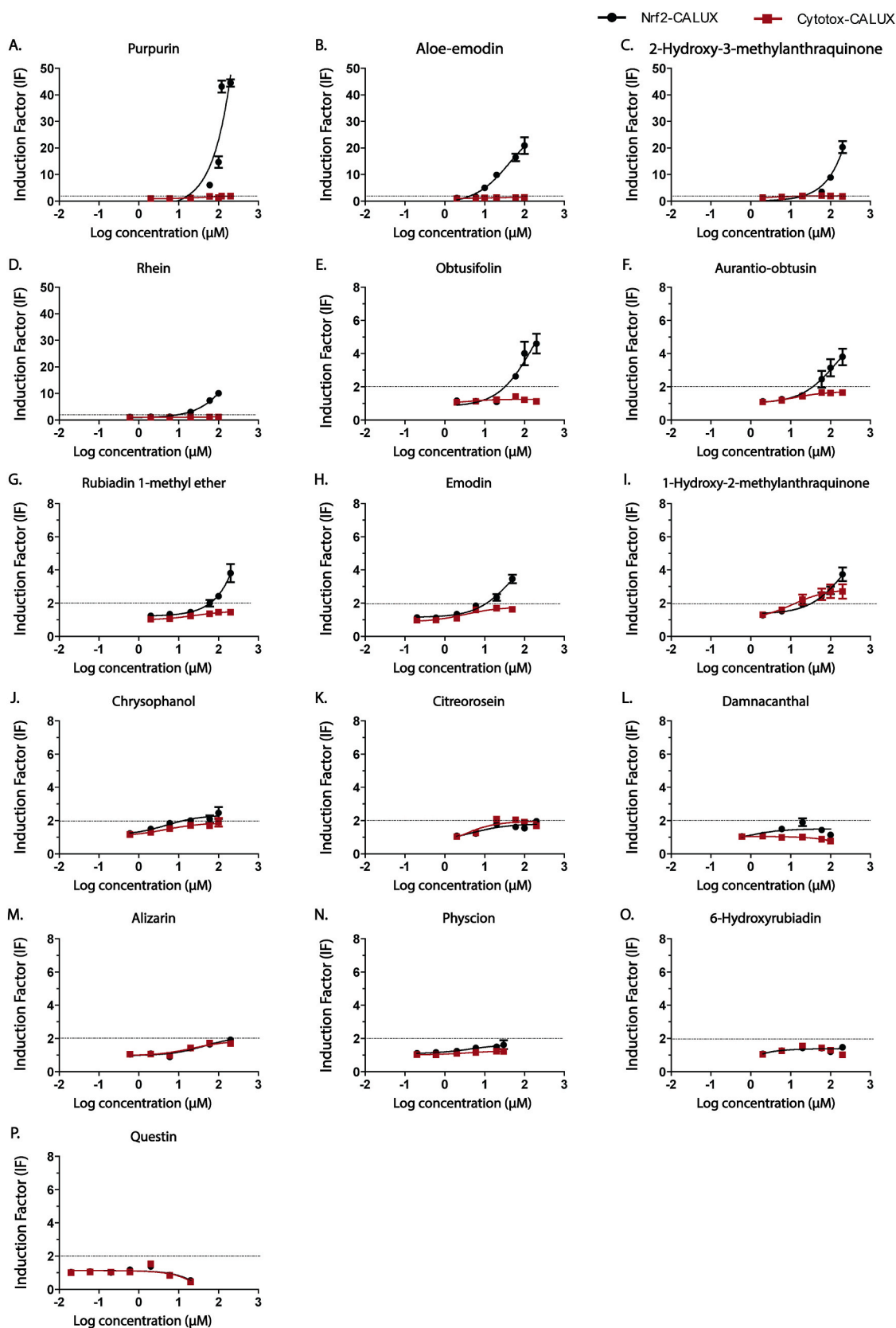


**Fig. 2.** Concentration dependent induction of luciferase activity in Nrf2 CALUX (black symbols) and Cytotox CALUX (red symbols) reporter cells after 24h-exposure to different hydroxyanthraquinones. Luciferase activity is expressed as induction factor (IF) compared to the solvent control. Data are presented as mean  $\pm$  SEM of at least three independent replicates. (For interpretation of the references to colour in this figure legend, the reader is referred to the Web version of this article.)

indicating that the induction was not due to hydroxyanthraquinone mediated stabilization of the produced luciferase protein. For purpurin and 2-hydroxy-3-methylanthraquinone a limited response in the Cytotox CALUX assay was observed (around IF of 2) while their induction in Nrf2 CALUX assay amounted up to IF of 50 and 20 for the highest concentrations tested. Nrf2 induction by obtusifolin, aurantio-obtusin, rubiadin 1-methyl ether and emodin (Fig. 2E–G), resulted in IFs that ranged from 3.4 to 4.6 for the highest concentration (200  $\mu$ M) tested. Also here the response could not be ascribed to stabilization of the luciferase expression. Fig. 2I–K illustrate that the Nrf2 induction by 1-hydroxy-2-methylanthraquinone, chrysophanol and citreorosein was limited and to some extent related to stabilization of the luciferase protein as reflected by the also limited concentration dependent increase of the IFs in the Cytotox CALUX assay. The other 5 hydroxyanthraquinones (Fig. 2L–P) did not induce Nrf2 mediated gene expression. While for quetin at the highest concentration tested some cytotoxicity was observed.

Benchmark dose (BMD) modelling was performed on the Nrf2 induction data that were corrected for the responses observed in the Cytotox Calux (see Fig. S2) to define the BMCL<sub>10</sub> values (Tables S1–S8). The BMCL<sub>10</sub> values are the lower 95% confidence limit of the concentration inducing 10% added effect above background. Because the concentration response curves showed no saturation the BMD modelling was performed using 10% added instead of 10% extra effect. The BMCL<sub>10</sub> values thus obtained amounted to 16  $\mu$ M for purpurin; 1.1  $\mu$ M for aloe emodin; 23  $\mu$ M for 2-hydroxy-3-methylanthraquinone; 2.3  $\mu$ M for rhein. 15  $\mu$ M for obtusifolin; 4.6  $\mu$ M for aurantio-obtusin; 9.8  $\mu$ M for rubiadin 1-methyl ether; and 3.8  $\mu$ M for emodin.

### 3.2. Induction of Nrf2 mediated gene expression by methanolic extracts from single herb-based granules and TCMs

The extracts of the selected single herb-based granules were tested in the Nrf2 CALUX and Cytotox CALUX reporter gene assays at 200  $\mu$ g/ml (1% v/v DMSO) and 400  $\mu$ g/ml (2% v/v DMSO) (Fig. 3A). Extracts from granules of Aloe, and Madder at the concentration of 200  $\mu$ g/ml were positive (IF > 2.0) in the Nrf2 CALUX reporter gene assay. Extracts from Rhubarb were cytotoxic at 200  $\mu$ g/ml, indicated by a lower IF obtained from the Cytotox CALUX assay compared to induction by the solvent control, although Rhubarb extracts induced Nrf2 CALUX (Fig. 3A).

Upon increasing the concentrations of the extracts to 400  $\mu$ g/ml all responses in the Nrf2 CALUX assay were higher compared to the responses observed at 200  $\mu$ g/ml. In addition to extracts from Aloe and Madder, also Polygonum and Cassia Seed induced a response in the Nrf2 CALUX assay at 400  $\mu$ g/ml while the responses in the Cytotox CALUX assay also minimally increased. The Rhubarb extract showed increased cytotoxicity at 400  $\mu$ g/ml compared to 200  $\mu$ g/ml as shown by the results of the Cytotox CALUX assay. The highest induction of the Nrf2 CALUX assay was observed for extracts of Madder (IF of 10.9), and Aloe (IF of 9.4).

The extracts of selected TCMs were also tested in both the Nrf2 CALUX and the Cytotox CALUX assays at 200  $\mu$ g/ml (1% v/v DMSO) and 400  $\mu$ g/ml (2% v/v DMSO) (Fig. 3B). At 200  $\mu$ g/ml, only the extract of CXLKYP induced Nrf2 mediated gene expression (IF of 4.9). When the extract concentrations were increased to 400  $\mu$ g/ml all tested TCM extracts induced Nrf2 mediated gene expression. Highest induction (IF of 22.6) was observed following exposure of 400  $\mu$ g/ml of the extract of CXLKYP.

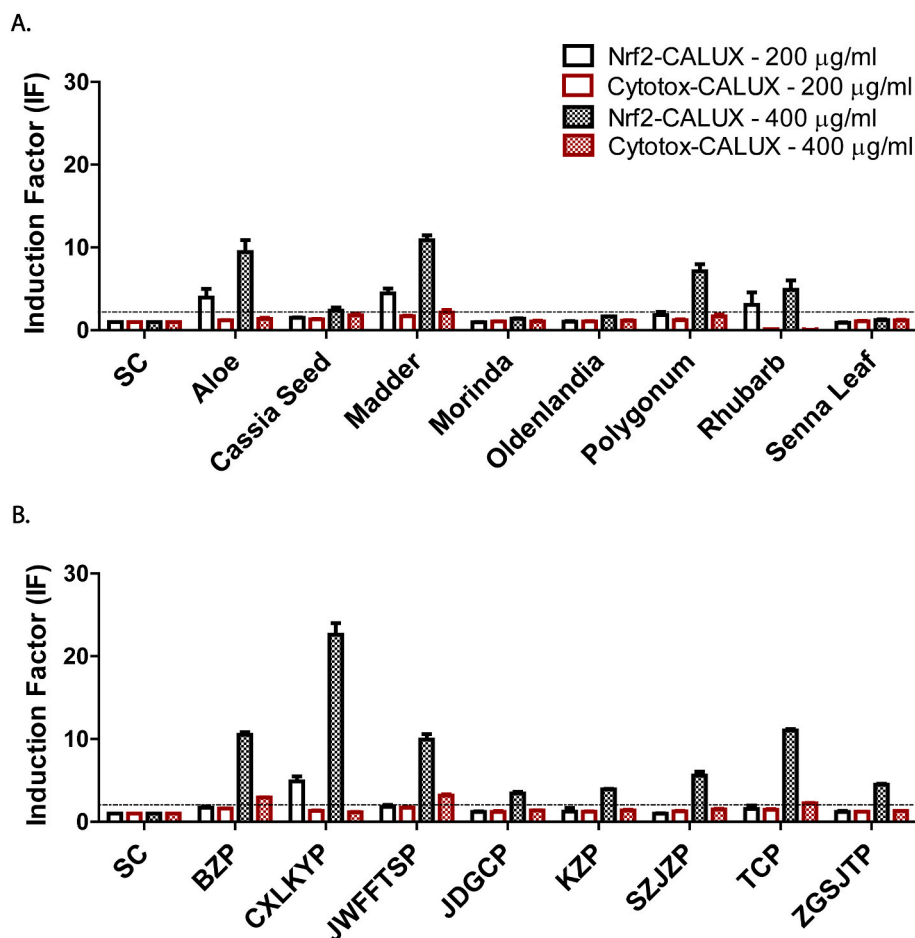


**Fig. 3.** Luciferase activity in Nrf2 CALUX and Cytotox CALUX assay measured after 24h exposure of the cells to extracts of selected single herb-based granules (A) and TCMs (B) at 200  $\mu$ g/ml and 400  $\mu$ g/ml; SC means solvent control (1% v/v DMSO or 2% v/v DMSO). The luciferase activity is expressed as induction factor (IF), compared to the solvent control. Dried methanolic extract of single herb-based granules/TCMs dissolved in DMSO at 20 mg/ml were added to exposure medium to give final concentrations of 200  $\mu$ g/ml and 400  $\mu$ g/ml with 1% (v/v) DMSO and 2% (v/v) final DMSO, respectively. Data are presented as mean  $\pm$  SEM of three independent replicates.

### 3.3. Expression of HO-1 gene induced by hydroxyanthraquinones in Nrf2 CALUX cells and wild type U2OS cells

To validate the results from the Nrf2 CALUX reporter gene assay, the expression of HO-1 induced by purpurin and aloë-emodin in Nrf2 CALUX cells and wild type U2OS cells was quantified by RT-qPCR at the (Fig. 4). This was done using 200  $\mu$ M purpurin and 100  $\mu$ M aloë-emodin, their respective highest concentration used in the Nrf2 CALUX reporter gene assay. In both the Nrf2 CALUX cell line and the wild type cell line, purpurin and aloë-emodin significantly upregulated the HO-1 gene expression. In the Nrf2 CALUX cell line, the fold induction of HO-1 mRNA expression by purpurin and aloë-emodin compared to control was 2.5 fold and 1.9 fold, respectively (Fig. 4A), while in the wild type U2OS cell line, the fold induction of HO-1 mRNA expression by purpurin and aloë-emodin compared to control was 5.3 fold and 3.5 fold, respectively (Fig. 4B).

### 3.4. Identification and quantification of 8 selected hydroxyanthraquinone inducers of Nrf2 mediated gene expression in methanolic extracts of single herb-based granules and TCMs

Fig. 5 and Table S10 present the levels of the hydroxyanthraquinones, which were shown to be Nrf2 inducers, in extracts of single herb-based granules and TCM. The results in Fig. 5A reveal that the extracts of aloë and rhubarb contain relatively high concentrations of total hydroxyanthraquinones, amounting to 11,341  $\mu$ g/g extract and 11,087  $\mu$ g/g extract, respectively. The results also reveal that in the aloë extract, aloë-emodin was identified as the major hydroxyanthraquinone (around 99% of total) while only 1% of the total concentration was present as rhein. In contrast, rhein was abundantly present in the extract of rhubarb (around 58% of total hydroxyanthraquinones) with additional hydroxyanthraquinones present in the rhubarb extract being emodin (around 23% of total), aloë-emodin (around 18% of total), purpurin and aurantio-obtusin (less than 1% of total). Extracts of Cassia Seed and Senna Leaf also contained substantial amounts of hydroxyanthraquinones, amounting to 3440  $\mu$ g/g extract and 3456  $\mu$ g/g extract, respectively. Aurantio-obtusin and emodin were detected as the major hydroxyanthraquinones in Cassia Seed extract while rhein was found to be a major hydroxyanthraquinone in Senna Leaf. Purpurin (around 94% of total) and rhein (around 6%) were detected in Madder extract and only emodin was found in Polygonum extract. Morinda and Oldenlandia appeared not to contain any of the targeted hydroxyanthraquinones.

Compared to extracts of single herb-based granules, extracts of TCM showed relatively lower concentrations of hydroxyanthraquinones as shown in Fig. 5B and Table S11. Among the eight TCM extracts analysed, BZP and TCP contained relatively higher levels of hydroxyanthraquinones, amounting to 4037  $\mu$ g/g extract and 3752  $\mu$ g/g extract, respectively. Aloë-emodin, emodin and rhein were detected in both these two extracts, and also, albeit at a somewhat lower level, in the extract of SZJZP.

As a final step we investigated to what extent the detected concentrations of hydroxyanthraquinones (converted to  $\mu$ M and presented in Table S12 and Table S13) in combination with the concentration response curves and BMCL<sub>10</sub> values for 10% added effect above background level of the Nrf2 induction by the individual compounds could account for the Nrf2 induction of the extracts of TCM and single herb-based granules. To this end RPF for every positive hydroxyanthraquinone were calculated (Table S14) and Fig. 6 presents a comparison of the experimentally observed IF of the various extracts tested at 400  $\mu$ g/ml (after correction for the response in the Cytotox CALUX assay) and the IF calculated based on the detected levels of the hydroxyanthraquinones and their relative potency compared to aloë-emodin, expressing the total hydroxyanthraquinone levels in the extracts in aloë-emodin equivalents and the corresponding IF as derived from the aloë-emodin concentration response curve. Fig. 6A shows that extracts of Aloë, Cassia Seed and Senna leaf display comparable IFs if calculated and determined experimentally at 400  $\mu$ g/ml. For the extracts of Polygonum and Madder, the concentrations of hydroxyanthraquinones were too low to contribute to Nrf2 induction. No IF could be calculated for Morinda and Oldenlandia as we did not detect the selected hydroxyanthraquinones in these products. The extract of Rhubarb was not compared here, since it displayed cytotoxicity at 400  $\mu$ g/ml.

As Fig. 6B showed, for extracts of BZP, SZJZP and TCP, their experimentally determined IFs were much higher than their respective calculated IFs. For extracts of JWFFTSP, JDGCP and KZP, they contained lower concentration of hydroxyanthraquinones at 400  $\mu$ g/ml, which cannot explain the observed Nrf2 induction. For CXLKYP and ZGSJTP, no IF could be calculated because no selected hydroxyanthraquinones was detected in them, while some activity on the Nrf2 CALUX assay was detected experimentally (Fig. 6B).

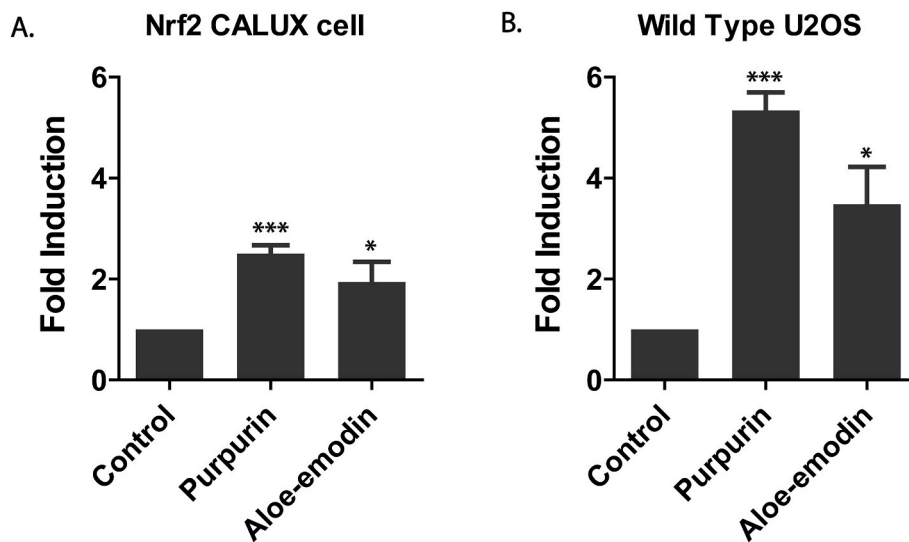


Fig. 4. Upregulation of HO-1 mRNA expression by purpurin (200  $\mu$ M) and aloë-emodin (100  $\mu$ M), in Nrf2 CALUX cells (A) and wild type U2OS cells (B). The results were expressed as fold induction compared to solvent control (1% v/v DMSO). Data are shown as mean  $\pm$  SEM of at least three independent replicates and \* indicates a response significantly different from treatment of solvent control (1% DMSO) (\*,  $p < 0.05$ ; \*\*,  $p < 0.01$ ; \*\*\*,  $p < 0.001$ ; Student's t-test).



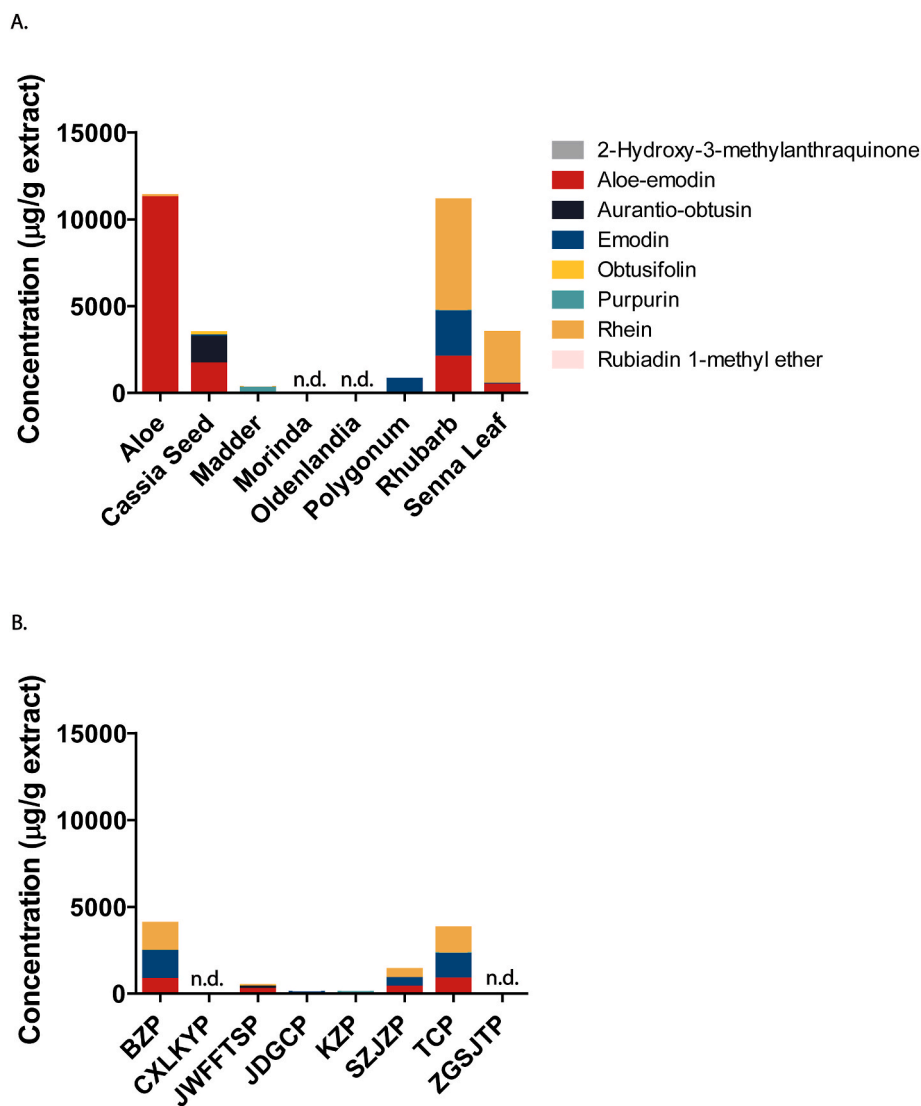
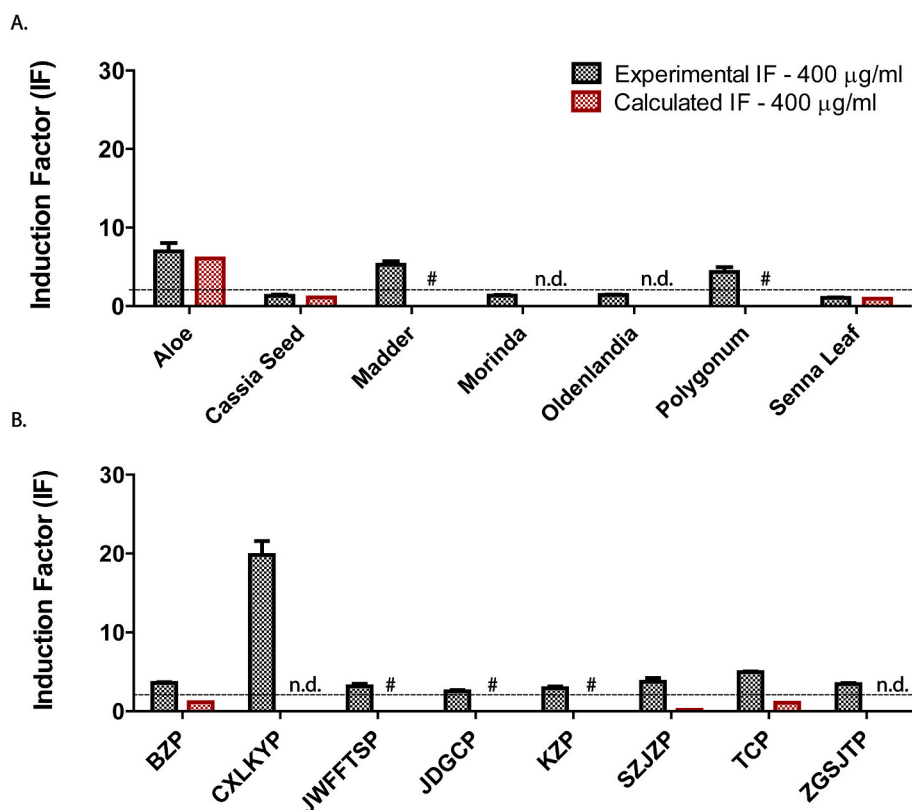


Fig. 5. Concentrations (µg/g extract) of 8 hydroxyanthraquinones as potential inducers of Nrf2 mediated gene expression in methanolic extracts of single herb-based granules (A) and TCM (B). "n.d.": no hydroxyanthraquinones detected in extract.

#### 4. Discussion

Traditional Chinese medicine (TCM) and individual herbs have claimed beneficial (intestinal) health effects and are thus frequently used as alternative treatments of several human intestinal complaints. The biological activity has been attributed to the presence of hydroxyanthraquinones in these TCM and herbs (Teschke et al., 2015; Zhang et al., 2020). Hydroxyanthraquinones can be found in numerous plant species belonging to different families (Gao et al., 2017; Hsu and Chung, 2012; Tessier et al., 1981; Wang et al., 2013, 2020; Zahn et al., 2008; Zhang et al., 2012). A growing number of studies focuses on the potential beneficial effects of several hydroxyanthraquinones such as rhein, emodin, aloe-emodin, including their potency to induce beneficial Nrf2 mediated gene expression (Antonisamy et al., 2019; Bu et al., 2018; Li et al., 2021; Park et al., 2016; Shang et al., 2021; Shen et al., 2022; Tian et al., 2018; Zhuang et al., 2019a, 2019b). However, for other hydroxyanthraquinones not much is known on their potential for Nrf2 induction. Here, we successfully used the Nrf2 CALUX reporter gene assay to investigate the potential of 16 individual hydroxyanthraquinones claimed to be present in plants and of extracts of selected TCMs and single herb-based granules for induction of Nrf2 mediated gene expression.

From the results obtained in the Nrf2 CALUX assay, 8 of the 16 hydroxyanthraquinones, including purpurin, aloe-emodin, 2-hydroxy-3-methylanthraquinone, rhein, aurantio-obtusin, obtusifolin, rubiadin-1-methyl ether and emodin were shown able to induce the Nrf2-EpRE mediated gene expression in the Nrf2 CALUX assay in a concentration-dependent manner. Among these 8 hydroxyanthraquinones, the maximum IFs of purpurin, aloe-emodin, 2-hydroxy-3-methylanthraquinone and rhein in the Nrf2 CALUX assay were 45.5, 20.9, 20.3 and 10.1, respectively (Fig. 2). Based on the concentration response curves obtained upon correction for the response in the Cytotox CALUX assay, BMCL<sub>10</sub> values for 10% added effect above background were calculated. Aloe-emodin and rhein induced Nrf2 mediated gene expression at lower concentrations (BMCL<sub>10</sub> of 1.1 µM and 2.3 µM, respectively) than purpurin and 2-hydroxy-3-methylanthraquinone (BMCL<sub>10</sub> of 16 µM, and 23 µM, respectively). Our findings about Nrf2 activation by purpurin, aloe-emodin and rhein confirms results from earlier studies in which purpurin (30 µM and 100 µM) effectively reversed the down-regulation of Nrf2 expression in mice hepatocytes after 0.1% alcohol treatment (Hussain et al., 2022). Aloe-emodin induced EpRE-mediated gene expression in an EpRE-LUX reporter gene assay at 20 µM (IF = 5) (Papadi et al., 2019), and aloe-emodin increase HO-1 expression in L02 and HepaRG cells at 40 µM (Hu et al., 2022). Rhein was found previously



**Fig. 6.** Comparison of calculated induction factor (IF) and experimental induction factor (IF) in the Nrf2 CALUX assay for dried methanolic extracts of single herb-based granules (A) and TCM (B) at 400 µg/ml. The calculated IF was obtained by expressing the total level of hydroxyanthraquinones present in each extract in aloe-emodin equivalents and then predicting the IF using the corrected concentration response curve for aloe-emodin. The experimental IF was the IF obtained in the Nrf2 CALUX assay after 24h incubation and correcting for the response in the Cytotox CALUX assay, and data are presented as mean ± SEM of three independent replicates. “#”: individual hydroxyanthraquinones detected in respective extract but the calculated IF was negligible. “n.d.”: no hydroxyanthraquinones detected in extract.

to induce the Nrf2-EpRE mediated gene expression upon 17h exposure at 4 µM in rat small intestine epithelial cells (IEC-6 cells) (Zhuang et al., 2019b). For the other 6 hydroxyanthraquinones acting as Nrf2 inducers, obtusifolin showed the highest IF of 4.60, followed by aurantio-obtusin, rubiadin 1-methyl ether and emodin, whose IFs were 3.80, 3.80 and 3.42, respectively. For 1-hydroxy-2-methylantraquinone, the IF in the Nrf2 CALUX assay reached 3.73 at 200 µM while its IF in Cytotox CALUX assay was also relatively high, indicating part of the activity may originate from stabilizing the luciferase protein. The results from BMD analysis showed obtusifolin, aurantio-obtusin and emodin had a comparable BMCL<sub>10</sub> of 15 µM, 4.6 µM and 3.8 µM, respectively. The Nrf2 activation by emodin was in line with results from previous studies. One study indicated that emodin was an Nrf2 inducer in mouse BV2 microglial cells after 2 h exposure at 40 µM (Park et al., 2016). Another in vitro study reported that emodin significantly induced Nrf2-luc activity and upregulated the downstream gene expression of antioxidant genes in rat neuron-like PC12 cells after 6-h exposure at concentrations from 10 µM to 30 µM (Ding et al., 2022). In addition to these in vitro studies, rhein and emodin induced Nrf2 and the downstream gene expression like heme oxygenase-1 in vivo studies, and showed antioxidant effect on brain and anti-inflammatory effects on intestine, liver and lung tissues (Antonisamy et al., 2019; Bu et al., 2018; Li et al., 2021; Shang et al., 2021; Shen et al., 2022; Tian et al., 2018; Zhuang et al., 2019b). We are the first to report that other hydroxyanthraquinones, 2-hydroxy-3-methylantraquinone, obtusifolin, aurantio-obtusin, and rubiadin 1-methyl ether were also able to induce Nrf2-EpRE mediated gene expression. For some hydroxyanthraquinones we observed both an induction of the Nrf2-EpRE-mediated gene expression and a concomitant increase in cytotoxicity observed with the Cytotox CALUX. The Cytotox CALUX assay serves as a control for cytotoxicity and non-specific activation or inhibition of luciferase expression (Auld et al., 2008; Thorne et al., 2010). Thus, the responses observed in the Nrf2 CALUX for 1-hydroxy-2-methylantraquinone, chrysophanol, citreosein and damnacanth were regarded as false positive for Nrf2-EpRE signaling pathway.

Besides, RT-qPCR was used to validate the results of the Nrf2 CALUX assay (Fig. 4). The two most potent compounds, purpurin and aloe-emodin were tested at the highest concentration at which they were tested in the Nrf2 CALUX assay. The results showed a significantly upregulated HO-1 gene expression in both Nrf2 CALUX cells and in the wild type cells used for the CALUX assay. The results are in line with the induction of luciferase gene expression in the Nrf2 CALUX assay. The higher fold induction detected when using luciferase activity as the read out in the Nrf2 CALUX assay as compared to the fold induction for HO-1 mRNA levels detected by RT-qPCR might be related to the fact that the Nrf2 CALUX cells contain the firefly luciferase gene under control of four EpRE, resulting in a more pronounced response.

The results obtained revealed that especially purpurin, with 3 hydroxyl moieties on one of its aromatic rings, showed a high potential for Nrf2 activation. Given that these hydroxyl substituents are electron donating groups this may point at a mode of action related to ionization and ROS formation rather than to electrophilicity as the mode of action underlying the Nrf2 induction, a novel finding that is of interest for future investigations.

In a next step a well-established modified methanolic extraction (Wei et al., 2013) was used in order to extract free hydroxyanthraquinones from herbs (i.e. single herb-based granules) and TCMs likely to contain these active ingredients. We selected single herb-based granules and TCMs that, based on previous studies and information on the labels could contain one or more hydroxyanthraquinones. Two concentrations of dried extracts (200 and 400 µg extract/ml) were assessed in the Nrf2 CALUX assay. And the same concentrations were evaluated in the Cytotox CALUX assay to exclude an interaction between the extract and the luciferase reporter protein, which could lead to false positive activity (Auld et al., 2008; Papadi et al., 2019; van der Linden et al., 2014). The concentrations were selected to enable detection of the intrinsic activity of the extracts to induce Nrf2 mediated gene expression, and to achieve active concentrations of individual ingredients that are present at only a fraction of the total concentration. The methanolic extract of Aloe and

Madder showed a high capacity for Nrf2 activation at both 200 µg/ml and 400 µg/ml in a concentration-dependent manner while Polygonum only induced Nrf2 mediated gene expression at 400 µg/ml (Fig. 3A). For Cassia Seed, the IF of Nrf2 CALUX assay at 400 µg/ml was over 2.0 fold while the response of the Cytotox CALUX assay also increased at this concentration (Fig. 3A). Therefore the Nrf2 response was regarded as a false positive one. LC-MS/MS results confirmed that the Nrf2 activation capacity of Aloe can be ascribed to the presence of hydroxyanthraquinones present in these extracts, assuming additive effects of the individual hydroxyanthraquinones present in this extract (Fig. 6A). However, for Madder that only contained low concentrations of purpurin and rhein and Polygonum containing emodin (Fig. 5A), this is not the case as the plant extracts showed higher Nrf2 induction than can be expected based on the concentration of the individual hydroxyanthraquinones (Fig. 6A), which means that the detected hydroxyanthraquinones in these two extracts of single herb-based granules only partly explain their Nrf2 induction. A previous study showed that Madder also contains mollugin which was reported to significantly activate the Nrf2 pathway and induce HO-1 expression (Devi Priya and Siril, 2014). Polygonum was previously found to contain Nrf2 inducers like 2, 3, 5, 4'-tetrahydroxystilbene-2-O-β-d glucoside (Lin et al., 2018, 2018, 2018; Yuan et al., 2020). While Cassia Seed and Senna leaf did contain hydroxyanthraquinones that as individual compound induced the Nrf2, the single herb-based extracts did not induce Nrf2 activation and thus the extracts cannot be regarded as Nrf2 inducers (IF < 2.0). The methanolic extract of the single herb-based granules Rhubarb showed strong cytotoxicity for U2OS cells at 200 µg/ml and 400 µg/ml, though it showed Nrf2 induction (Fig. 3A), which can be caused by the unknown presence of other chemicals.

All of our tested methanolic extracts of TCM induced the Nrf2 mediated gene expression at a concentration of 400 µg/ml (Fig. 3B). While the fold induction of the Nrf2 mediated gene expression by extracts of TCM did not always correspond with the concentration of the detected hydroxyanthraquinones. CXLKYP activated Nrf2 mediated gene expression, while we did not observe any of our positive hydroxyanthraquinones in this extract by LC-MS/MS (Fig. 5B). A previous study reported that some other plants used in CXLKYP, for example, *Andrographis paniculate* contained andrographolide (a labdane diterpenoid) which is known to significantly induce the Nrf2 signaling pathway (Seo et al., 2017; Wong et al., 2016). And *Taraxacum officinale* and *Prunella vulgaris* present in this TCM were also reported to induce the Nrf2 signaling pathway (Dong et al., 2020; Huang et al., 2018; Hwang et al., 2012). Similarly extracts from ZGSJTP, induced Nrf2 mediated gene expression while we did not detect our hydroxyanthraquinones in this extract. Clematichinenoside as an active compound in *Clematis chinensis*, which is a herb included in ZGSJTP enhanced the hypoxia/reoxygenation (H/R) stimulated activation of the Nrf2/HO-1 signaling pathway in HK-2 cells (Feng et al., 2020). And curcumin as a major active compound in the rhizome of *Curcuma longa* (also an ingredient in this TCM) activates Nrf2 significantly (Reuland et al., 2013). And another four plant ingredients, *Commiphora myrrha*, *Spatholobus suberectus*, root of *Rehmannia glutinosa* and root of *Ligusticum chuanxiong* in ZGSJTP are also reported to induce Nrf2 activation (Do et al., 2018; Lebda et al., 2021; Liu et al., 2020; Mengmeng Wang et al., 2021b). For methanolic extracts of BZP, TCP and SZJZP, aloe-emodin, emodin and rhein were the major hydroxyanthraquinones detected at relatively high concentrations in our study (Fig. 5B). However, the calculated Nrf2 activation is lower than the experimentally determined Nrf2 activation by the individual hydroxyanthraquinones present in the extracts. This can be explained by previous studies which reported that BZP contained many active compounds as potential Nrf2 inducers, such as plantamajoside in *Plantago asiatica*, Juglanin in *Polygonum aviculare*, Geniposide and Crocetin in *Gardenia jasminoides*, 3-aryl coumarin liquiriticoumarin and crotiliquiritin in *Glycyrrhiza uralensis* (Kong and Xu, 2020; Nguyen et al., 2021; Shen et al., 2020; Miaomiao Wang et al., 2021c; Wen et al., 2021; Zeng et al., 2022). TCP contains potential Nrf2 inducers, such as

*Prunus Persica* Seeds, Z-ligustilide (a benzoquinone derivative) in radix of *Angelica* and notopteron in *Notopterygium incisum* (Chen et al., 2021; Peng et al., 2013; Rehman et al., 2022). The ingredients of SZJZP, such as the *Salvia miltiorrhiza* containing cryptotanshinone and tanshinone, were also reported to induce Nrf2 activation (Nagappan et al., 2019; Tao et al., 2013).

The extract of JWFFTSP displayed a relatively high induction of Nrf2 mediated gene expression (Fig. 3B), though it only showed relatively low concentrations of aloe-emodin, aurantio-obtusin, rhein and obtusifolin (Fig. 5B). The presence of other ingredients in it, for instance, *Cinnamomum cassia* that was previously reported as a inducer of Nrf2-EpRE-mediated gene expression can explain this difference (Wondrak et al., 2010). JDGCP and KZP contained small amount of hydroxyanthraquinones that were only minimally able to induce Nrf2 mediated gene expression while in these extracts the activity may originate not only from hydroxyanthraquinones but also from ingredients from other plant constituents of the TCM, such as *Lycium barbarum*, *Polygonatum sibiricum*, *Ganoderma lucidum*, rhizome of *Alisma orientale*, *Curcuma longa* containing curcumin, *Carthamus tinctorius*, *Angelica sinensis* and *Ligusticum chuanxiong* in JDGCP as well as *Scutellaria barbata*, *Coix lacryma-jobi* containing 4-ketopinoselin and *Paris polyphylla* containing curcumin from KZP (Ashrafzadeh et al., 2020; Cao et al., 2017; Chen et al., 2012; Han et al., 2013; Li et al., 2020; Man et al., 2016; Su et al., 2020; Wang et al., 2021a,c; Y. Wang et al., 2019; Wu et al., 2013; Zhang et al., 2021).

## 5. Conclusion

In the present study, a high-throughput method, the Nrf2 CALUX reporter gene assay combined with the Cytotox CALUX assay, was used to quantify the concentration dependent Nrf2 activation by a series of hydroxyanthraquinones and several extracts of single herb-based granules and TCM. The results obtained reveal that 8 of 16 individual hydroxyanthraquinones including purpurin, aloe-emodin, 2-hydroxy-3-methylanthraquinone, rhein, obtusifolin, aurantio-obtusin, rubiadin 1-methyl ether and emodin induce Nrf2 mediated gene expression with BMCL<sub>10</sub> values in the low µM concentration range. Methanolic extracts from Aloe, Cassia Seed, Madder, and Polygonum also showed concentration-dependent induction of Nrf2. And all TCM extracts tested induced Nrf2-EpRE mediated gene expression. The Nrf2 induction was confirmed by RT-PCR measurement of HO-1 gene expression induced by purpurin and aloe-emodin. Subsequent LC-MS/MS based quantification of the levels of the hydroxyanthraquinones that were shown to be active Nrf2 inducers in the extracts revealed that the Nrf2 induction by the extracts could be partially, but not fully, explained by the presence of these hydroxyanthraquinones. Identification of additional Nrf2 inducers in these extracts, like for example flavonoids (Cao et al., 1997; Elbandy et al., 2014; López et al., 2013), remains of interest for future studies. Further studies could also involve omics based analysis to identify the whole pattern of downstream effects following the Nrf2 EpRE pathway induction by hydroxyanthraquinones as done for other Nrf2 inducers (Liu et al., 2022; Otsuki et al., 2021; Quiles et al., 2017; Shelton et al., 2015). Lastly, it is of interest to study the mode of action underlying the Nrf2 activation by the hydroxyanthraquinones in some more detail given that in theory these compounds could exert both electrophilic reactivity as well as redox cycling capacity producing reactive oxygen species and oxidative stress.

## CRedit authorship contribution statement

**Qihui Ren:** Conceptualization, Investigation, Writing – original draft, Visualization. **Wouter Bakker:** Methodology, Writing – review & editing. **Laura de Haan:** Methodology. **Ivonne M.C.M. Rietjens:** Conceptualization, Writing – review & editing, Supervision. **Hans Bouwmeester:** Conceptualization, Writing – review & editing, Supervision.

## Declaration of competing interest

The authors declare that they have no known competing financial interests or personal relationships that could have appeared to influence the work reported in this paper.

## Data availability

Data will be made available on request.

## Acknowledgement

This work was supported by a grant from the China Scholarship Council (No. 201906890022) to Qihui Ren. The authors acknowledge Biodetection Systems (BDS, Amsterdam) for providing the Nrf2 CALUX reporter gene cells.

## Appendix A. Supplementary data

Supplementary data to this article can be found online at <https://doi.org/10.1016/j.fct.2023.113802>.

## References

- Ahmed, S.M.U., Luo, L., Namani, A., Wang, X.J., Tang, X., 2017. Nrf2 signaling pathway: pivotal roles in inflammation. *Biochim. Biophys. Acta (BBA) - Mol. Basis Dis.* 1863, 585–597. <https://doi.org/10.1016/j.bbadis.2016.11.005>.
- Ahuja, M., Kaidery, N.A., Dutta, D., Attucks, O.C., Kazakov, E.H., Gazaryan, I., Matsumoto, M., Igarashi, K., Sharma, S.M., Thomas, B., 2022. Harnessing the therapeutic potential of the nrf2/bach1 signaling pathway in Parkinson's disease. *Antioxidants* 11, 1780. <https://doi.org/10.3390/antiox11091780>.
- Akbar, S., 2020. *Rheum officinale* baill.; *R. Palmatum* L. (Polygonaceae). In: *Handbook of 200 Medicinal Plants*. Springer International Publishing, Cham, pp. 1527–1537. [https://doi.org/10.1007/978-3-030-16807-0\\_158](https://doi.org/10.1007/978-3-030-16807-0_158).
- Alehaideb, Z., Chin, K.C., Yao, M.C., Law, F.C.P., 2019. Predicting the content of anthraquinone bioactive in *Rhei rhizoma* (*Rheum officinale* Baill.) with the concentration addition model. *Saudi Pharmaceut. J.* 27, 25–32. <https://doi.org/10.1016/j.jsps.2018.07.015>.
- Ali, M.Y., Park, S., Chang, M., 2021. Phytochemistry, ethnopharmacological uses, biological activities, and therapeutic applications of *Cassia obtusifolia* L.: a comprehensive review. *Molecules* 26, 6252. <https://doi.org/10.3390/molecules26206252>.
- Anh, V.T.P., Van Minh, V., Tuan, V.C., Van Khanh, N., Dung, D.T., Nhiem, N.X., Van Kiem, P., 2021. Iridoids and anthraquinones from the roots of *Morinda officinalis*. *Vietnam Journal of Chemistry* 59, 27–31. <https://doi.org/10.1002/vjch.202006082>.
- Antonisamy, P., Agastian, P., Kang, C.-W., Kim, N.S., Kim, J.-H., 2019. Anti-inflammatory activity of rhein isolated from the flowers of *Cassia fistula* L. and possible underlying mechanisms. *Saudi J. Biol. Sci.* 26, 96–104. <https://doi.org/10.1016/j.sjbs.2017.04.011>.
- Ashrafizadeh, M., Ahmadi, Z., Mohammadinejad, R., Farkhondeh, T., Samarghandian, S., 2020. Curcumin activates the Nrf2 pathway and induces cellular protection against oxidative injury. *Corpus Mensurab. Music. (CMM)* 20, 116–133. <https://doi.org/10.2174/1566524019666191016150757>.
- Auld, D.S., Thorne, N., Nguyen, D.-T., Inglesse, J., 2008. A specific mechanism for nonspecific activation in reporter-gene assays. *ACS Chem. Biol.* 3, 463–470. <https://doi.org/10.1021/cb8000793>.
- Baba, M.Z., Gomathy, S., Wahedi, U., 2022. Role of Nrf2 pathway activation in neurological disorder: a brief review. *J. Pharmacol. Pharmacother.* 13, 229–238. <https://doi.org/10.1177/0976500X221128855>.
- Balachandran, P., Ibrahim, M.A., Zhang, J., Wang, M., Pasco, D.S., Muhammad, I., 2021. Crosstalk of cancer signaling pathways by cyclic hexapeptides and anthraquinones from *Rubia cordifolia*. *Molecules* 26, 735. <https://doi.org/10.3390/molecules26030735>.
- Bu, T., Wang, C., Meng, Q., Huo, X., Sun, H., Sun, P., Zheng, S., Ma, X., Liu, Z., Liu, K., 2018. Hepatoprotective effect of rhein against methotrexate-induced liver toxicity. *Eur. J. Pharmacol.* 834, 266–273. <https://doi.org/10.1016/j.ejphar.2018.07.031>.
- Cao, G., Sofic, E., Prior, R.L., 1997. Antioxidant and prooxidant behavior of flavonoids: structure-activity relationships. *Free Radic. Biol. Med.* 22, 749–760. [https://doi.org/10.1016/S0891-5849\(96\)00351-6](https://doi.org/10.1016/S0891-5849(96)00351-6).
- Cao, S., Du, J., Hei, Q., 2017. *Lycium barbarum* polysaccharide protects against neurotoxicity via the Nrf2/HO-1 pathway. *Exp. Ther. Med.* <https://doi.org/10.3892/etm.2017.5127>.
- Chen, H.-H., Chen, Y.-T., Huang, Y.-W., Tsai, H.-J., Kuo, C.-C., 2012. 4-Ketopinoresinol, a novel naturally occurring ARE activator, induces the Nrf2/HO-1 axis and protects against oxidative stress-induced cell injury via activation of PI3K/AKT signaling. *Free Radic. Biol. Med.* 52, 1054–1066. <https://doi.org/10.1016/j.freeradbiomed.2011.12.012>.
- Chen, M., Nan, T.-G., Xin, J., Cui, L., Zhang, B., Wang, X., Wang, B.-M., 2020. Development of an enzyme-linked immunosorbent assay method for the detection of rhein in *Rheum officinale*. *International Journal of Analytical Chemistry* 1–7. <https://doi.org/10.1155/2020/4294826>, 2020.
- Chen, D., Wang, Q., Li, Y., Sun, P., Kuek, V., Yuan, J., Yang, J., Wen, L., Wang, H., Xu, J., Chen, P., 2021. Notopterol attenuates estrogen deficiency-induced osteoporosis via repressing RANKL signaling and reactive oxygen species. *Front. Pharmacol.* 12, 664836. <https://doi.org/10.3389/fphar.2021.664836>.
- Choi, B., Kim, Y., Choi, J.S., Lee, H.J., Lee, C.J., 2019. Obtusifolin isolated from the seeds of *Cassia obtusifolia* regulates the gene expression and production of MUC5AC mucin in airway epithelial cells via affecting NF- $\kappa$ B pathway. *Phytother. Res.* 33, 919–928. <https://doi.org/10.1002/ptr.6284>.
- de Oliveira, M.R., de Souza, I.C.C., Brasil, F.B., 2021. Mitochondrial protection and anti-inflammatory effects induced by emodin in the human neuroblastoma SH-SY5Y cells exposed to hydrogen peroxide: involvement of the AMPK/Nrf2 signaling pathway. *Neurochem. Res.* 46, 482–493. <https://doi.org/10.1007/s11064-020-03181-1>.
- Deshmukh, P., Unni, S., Krishnappa, G., Padmanabhan, B., 2017. The Keap1–Nrf2 pathway: promising therapeutic target to counteract ROS-mediated damage in cancers and neurodegenerative diseases. *Biophys. Rev.* 9, 41–56. <https://doi.org/10.1007/s12551-016-0244-4>.
- Devi Priya, M., Siril, E.A., 2014. Traditional and modern use of indian madder (*Rubia cordifolia* L.): an overview. *Int. J. Pharmaceut. Sci. Rev. Res.* 25, 154–164. <https://doi.org/10.3389/fphar.2022.965390>.
- Ding, Z., Da, H. hong, Osama, A., Xi, J., Hou, Y., Fang, J., 2022. Emodin ameliorates antioxidant capacity and exerts neuroprotective effect via PKM2-mediated Nrf2 transactivation. *Food Chem. Toxicol.* 160, 112790. <https://doi.org/10.1016/j.fct.2021.112790>.
- Do, M., Hur, J., Choi, J., Kim, Y., Park, H.-Y., Ha, S., 2018. *Spatholobus suberectus* ameliorates diabetes-induced renal damage by suppressing advanced glycation end products in db/db mice. *Indian J. Manag. Sci.* 19, 2774. <https://doi.org/10.3390/ijms19092774>.
- Dong, L., Dongzhi, Z., Jin, Y., Kim, Y.-C., Lee, D.-S., Huang, S., Panichayupakaranant, P., Li, B., 2020. *i>/i>Taraxacum officinale</i> wigg. Attenuates inflammatory responses in murine microglia through the Nrf2/HO-1 and NF- $\kappa$ B signaling pathways. *Am. J. Chin. Med.* 48, 445–462. <https://doi.org/10.1142/S0192415X20500238>.*
- EFSA Panel on Food Additives and Nutrient Sources added to Food (ANS), Younes, M., Aggett, P., Aguilar, F., Crebelli, R., Filipič, M., Frutos, M.J., Galtier, P., Gott, D., Gundert-Remy, U., Kuhnle, G.G., Lambré, C., Leblanc, J., Lillegaard, I.T., Moldeus, P., Mortensen, A., Oskarsson, A., Stankovic, I., Waalkens-Berendsen, I., Woutersen, R.A., Andrade, R.J., Fortes, C., Mosesso, P., Restani, P., Pizzo, F., Smeraldi, C., Papaioannou, A., Wright, M., 2018. Safety of hydroxyanthracene derivatives for use in food. *EFSA Journal* 16. doi:10.2903/j.efsa.2018.5090.
- Elbandy, M.A., Abed, S.M., Gad, S.S.A., Abdel-Fadeel, M.G., 2014. Aloe Vera Gel as a Functional Ingredient and Natural Preservative in Mango Nectar.
- Fan, J.J., Li, C.H., Hu, Y.J., Chen, H., Yang, F.Q., 2018. Comparative assessment of in vitro thrombolytic and fibrinolytic activity of four aloe species and analysis of their phenolic compounds by LC-MS. *South Afr. J. Bot.* 119, 325–334. <https://doi.org/10.1016/j.sajb.2018.10.001>.
- Feng, J., Kong, R., Xie, L., Lu, W., Zhang, Y., Dong, H., Jiang, H., 2020. Clemaichinenoside protects renal tubular epithelial cells from hypoxia/reoxygenation injury in vitro through activating the Nrf2/HO-1 signalling pathway. *Clin. Exp. Pharmacol. Physiol.* 47, 495–502. <https://doi.org/10.1111/1440-1681.13219>.
- Gao, L., Xu, X., Yang, J., 2017. Anthraquinone and naphthoquinone derivatives from the root of *Rheum officinale*. *Chem. Nat. Compd.* 53, 1160–1162. <https://doi.org/10.1007/s10600-017-2225-7>.
- Gong, X.-P., Sun, Y.-Y., Chen, W., Guo, X., Guan, J.-K., Li, D.-Y., Du, G., 2017. Anti-diarrheal and anti-inflammatory activities of aqueous extract of the aerial part of *Rubia cordifolia*. *BMC Compl. Alternative Med.* 17, 20. <https://doi.org/10.1186/s12906-016-1527-9>.
- Gu, W., Yang, M., Bi, Q., Zeng, L.-X., Wang, X., Dong, J.-C., Li, F.-J., Yang, X.-X., Li, J.-P., Yu, J., 2020. Water extract from processed Polygonum multiflorum modulate gut microbiota and glucose metabolism on insulin resistant rats. *BMC Complement Med Ther* 20, 107. <https://doi.org/10.1186/s12906-020-02897-5>.
- Guo, R., Wu, H., Yu, X., Xu, M., Zhang, X., Tang, L., Wang, Z., 2017. Simultaneous determination of seven anthraquinone aglycones of crude and processed semen cassiae extracts in rat plasma by UPLC-MS/MS and its application to a comparative pharmacokinetic study. *Molecules* 22, 1803. <https://doi.org/10.3390/molecules22111803>.
- Han, C.W., Kwun, M.J., Kim, K.H., Choi, J.-Y., Oh, S.-R., Ahn, K.-S., Lee, J.H., Joo, M., 2013. Ethanol extract of *Alismatis Rhizoma* reduces acute lung inflammation by suppressing NF- $\kappa$ B and activating Nrf2. *J. Ethnopharmacol.* 146, 402–410. <https://doi.org/10.1016/j.jep.2013.01.010>.
- Hou, J., Gu, Y., Zhao, S., Huo, M., Wang, S., Zhang, Y., Qiao, Y., Li, X., 2018. Anti-inflammatory effects of aurantio-obtusin from seed of *Cassia obtusifolia* L. Through modulation of the NF- $\kappa$ B pathway. *Molecules* 23, 3093. <https://doi.org/10.3390/molecules23123093>.
- Hsu, S.-C., Chung, J.-G., 2012. Anticancer potential of emodin. *Biomedicine* 2, 108–116. <https://doi.org/10.1016/j.biomed.2012.03.003>.
- Hu, Y., Huang, W., Luo, Y., Xiang, L., Wu, J., Zhang, Y., Zeng, Y., Xu, C., Meng, X., Wang, P., 2021. Assessment of the anti-inflammatory effects of three rhubarb anthraquinones in LPS-Stimulated RAW264.7 macrophages using a pharmacodynamic model and evaluation of the structure-activity relationships. *J. Ethnopharmacol.* 273, 114027. <https://doi.org/10.1016/j.jep.2021.114027>.
- Hu, Y., Quan, Z., Li, D., Wang, C., Sun, Z., 2022. Inhibition of CYP3A4 enhances aloe-emodin induced hepatocyte injury. *Toxicol. Vitro* 79, 105276. <https://doi.org/10.1016/j.tiv.2021.105276>.



- Huang, S., Meng, N., Liu, Z., Guo, L., Dong, L., Li, B., Ye, Q., 2018. Neuroprotective effects of *Taraxacum officinale* wigg. Extract on glutamate-induced oxidative stress in HT22 cells via HO-1/Nrf2 pathways. *Nutrients* 10, 926. <https://doi.org/10.3390/nu10070926>.
- Hussain, Y., Singh, J., Raza, W., Meena, A., Rajak, S., Sinha, R.A., Luqman, S., 2022. Purpurin ameliorates alcohol-induced hepatotoxicity by reducing ROS generation and promoting Nrf2 expression. *Life Sci.* 309, 120964 <https://doi.org/10.1016/j.lfs.2022.120964>.
- Hwang, S.M., Lee, Y.J., Yoon, J.J., Lee, S.M., Kim, J.S., Kang, D.G., Lee, H.S., 2012. *Prunella vulgaris* suppresses HG-induced vascular inflammation via Nrf2/HO-1/eNOS activation. *Indian J. Manag. Sci.* 13, 1258–1268. <https://doi.org/10.3390/ijms13011258>.
- Kong, Y., Xu, S., 2020. Juglanin administration protects skin against UVB-induced injury by reducing Nrf2-dependent ROS generation. *Int. J. Mol. Med.* 46, 67–82. <https://doi.org/10.3892/ijmm.2020.4589>.
- Lebda, M.A., Mostafa, R.E., Taha, N.M., Abd El-Maksoud, E.M., Tohamy, H.G., Al Jaouni, S.K., El-Far, A.H., Elfeky, M.S., 2021. Commiphora myrrh supplementation protects and cures ethanol-induced oxidative alterations of gastric ulceration in rats. *Antioxidants* 10, 1836. <https://doi.org/10.3390/antiox10111836>.
- Li, Y., Jiang, J.-G., 2018. Health functions and structure–activity relationships of natural anthraquinones from plants. *Food Funct.* 9, 6063–6080. <https://doi.org/10.1039/C8FO01569D>.
- Li, Z., Bi, H., Jiang, H., Song, J., Meng, Q., Zhang, Y., Fei, X., 2020. Neuroprotective effect of emodin against Alzheimer's disease via Nrf2 signaling in U251 cells and APP/PS1 mice. *Mol. Med. Rep.* 23, 108. <https://doi.org/10.3892/mmr.2020.11747>.
- Li, G.-M., Chen, J.-R., Zhang, H.-Q., Cao, X.-Y., Sun, C., Peng, F., Yin, Y.-P., Lin, Z., Yu, L., Chen, Y., Tang, Y.-L., Xie, X.-F., Peng, C., 2021. Update on pharmacological activities, security, and pharmacokinetics of rhein. *Evid. base Compl. Alternative Med.* 2021, 1–18. <https://doi.org/10.1155/2021/4582412>.
- Lin, E.-Y., Bayarsengee, U., Wang, C.-C., Chiang, Y.-H., Cheng, C.-W., 2018. The natural compound 2,3,5,4'-tetrahydroxystilbene-2-O- $\beta$ -D-glucoside protects against adriamycin-induced nephropathy through activating the Nrf2-Keap1 antioxidant pathway. *Environ. Toxicol.* 33, 72–82. <https://doi.org/10.1002/tox.22496>.
- Lin, H., Chen, X., Zhang, C., Yang, T., Deng, Z., Song, Y., Huang, L., Li, F., Li, Q., Lin, S., Jin, D., 2021. EF24 induces ferroptosis in osteosarcoma cells through HMOX1. *Biomed. Pharmacother.* 136, 111202 <https://doi.org/10.1016/j.biopha.2020.111202>.
- Liu, Y., Mapa, M.S.T., Sprando, R.L., 2020. Liver toxicity of anthraquinones: a combined in vitro cytotoxicity and in silico reverse dosimetry evaluation. *Food Chem. Toxicol.* 140, 111313 <https://doi.org/10.1016/j.fct.2020.111313>.
- Liu, C., Boeren, S., Miro Estruch, I., Rietjens, I.M.C.M., 2022. The gut microbial metabolite pyrogallol is a more potent inducer of nrf2-associated gene expression than its parent compound green tea (-)-Epigallocatechin gallate. *Nutrients* 14, 3392. <https://doi.org/10.3390/nu14163392>.
- Livak, K.J., Schmittgen, T.D., 2001. Analysis of relative gene expression data using real-time quantitative PCR and the 2<sup>-</sup> $\Delta\Delta$ CT method. *Methods* 25, 402–408. <https://doi.org/10.1006/meth.2001.1262>.
- López, A., de Tangil, M., Vega-Orellana, O., Ramírez, A., Rico, M., 2013. Phenolic constituents, antioxidant and preliminary antimycoplasmic activities of leaf skin and flowers of aloe vera (*L. burm. F.* (syn. *A. barbadensis* mill.) from the canary islands (Spain). *Molecules* 18, 4942–4954. <https://doi.org/10.3390/molecules18054942>.
- Man, S., Li, J., Liu, J., Chai, H., Liu, Z., Wang, J., Gao, W., 2016. Curcumin alleviated the toxic reaction of *Rhizoma Paridis* saponins in a 45-day subchronic toxicological assessment of rats. *Environ. Toxicol.* 31, 1935–1943. <https://doi.org/10.1002/tox.22194>.
- Meier, N., Meier, B., Peter, S., Wolfram, E., 2017. In-Silico UHPLC method optimization for aglycones in the herbal laxatives aloe barbadensis mill., *Cassia angustifolia* vahl pods, *rhamnus frangula* L. Bark, *rhamnus purshianus* DC. Bark, and *Rheum palmatum* L. Roots. *Molecules* 22, 1838. <https://doi.org/10.3390/molecules22111838>.
- Miyazawa, M., Kawata, J., 2006. Identification of the key aroma compounds in dried roots of *Rubia cordifolia*. *J. Oleo Sci.* 55, 37–39. <https://doi.org/10.5650/jos.55.37>.
- Muzolf-Panek, M., Gliszczyńska-Swigoł, A., de Haan, L., Aarts, J.M.M.J.G., Szymusiak, H., Vervoort, J.M., Tyrakowska, B., Rietjens, I.M.C.M., 2008. Role of catechin quinones in the induction of EPRE-mediated gene expression. *Chem. Res. Toxicol.* 21, 2352–2360. <https://doi.org/10.1021/tx8001498>.
- Nagappan, A., Kim, J.-H., Jung, D.Y., Jung, M.H., 2019. Cryptotanshinone from the *Salvia miltiorrhiza* bunge attenuates ethanol-induced liver injury by activation of AMPK/SIRT1 and Nrf2 signaling pathways. *Indian J. Manag. Sci.* 21, 265. <https://doi.org/10.3390/ijms21010265>.
- Nguyen, L.T.H., Ahn, S.H., Nguyen, U.T., Yang, I.J., Shin, H.M., 2021. Geniposide, a principal component of gardeniae fructus, protects skin from diesel exhaust particulate matter-induced oxidative damage. *Evid. base Compl. Alternative Med.* 2021, 1–12. <https://doi.org/10.1155/2021/8847358>.
- Otsuki, A., Okamura, Y., Aoki, Y., Ishida, N., Kumada, K., Minegishi, N., Katsuoka, F., Kinoshita, K., Yamamoto, M., 2021. Identification of dominant transcripts in oxidative stress response by a full-length transcriptome analysis. *Mol. Cell Biol.* 41, e00472 <https://doi.org/10.1128/MCB.00472-20>.
- Papadi, G., Wesseling, S., Troganis, A.N., Vervoort, J., Rietjens, I.M.C.M., 2019. Induction of EPRE-mediated gene expression by a series of mediterranean botanicals and their constituents. *J. Ethnopharmacol.* 240, 111940 <https://doi.org/10.1016/j.jep.2019.111940>.
- Park, S.Y., Jin, M.L., Ko, M.J., Park, G., Choi, Y.-W., 2016. Anti-neuroinflammatory effect of emodin in LPS-stimulated microglia: involvement of AMPK/Nrf2 activation. *Neurochem. Res.* 41, 2981–2992. <https://doi.org/10.1007/s11064-016-2018-6>.
- Paudel, P., Jung, H.A., Choi, J.S., 2018. Anthraquinone and naphthopyrone glycosides from *Cassia obtusifolia* seeds mediate hepatoprotection via Nrf2-mediated HO-1 activation and MAPK modulation. *Arch Pharm. Res. (Seoul)* 41, 677–689. <https://doi.org/10.1007/s12272-018-1040-4>.
- Peng, B., Zhao, P., Lu, Y.-P., Chen, M.-M., Sun, H., Wu, X.-M., Zhu, L., 2013. Z-ligustilide activates the Nrf2/HO-1 pathway and protects against cerebral ischemia–reperfusion injury in vivo and in vitro. *Brain Res.* 1520, 168–177. <https://doi.org/10.1016/j.brainres.2013.05.009>.
- Quiles, J.M., Narasimhan, M., Shanmugam, G., Milash, B., Hoidal, J.R., Rajasekaran, N. S., 2017. Differential regulation of miRNA and mRNA expression in the myocardium of Nrf2 knockout mice. *BMC Genom.* 18, 509. <https://doi.org/10.1186/s12864-017-3875-3>.
- Rahman, MdM., Amin, R., Afroz, T., Das, J., 2021. Pharmaceutical, therapeutically and nutraceutical potential of aloe vera: a mini-review. *JPRI* 109–118. <https://doi.org/10.9734/jpri/2021/v33i37A31986>.
- Rehman, S., Nazar, R., Butt, A.M., Ijaz, B., Tasawar, N., Sheikh, A.K., Shahid, I., Shah, S. M., Qamar, R., 2022. Phytochemical screening and protective effects of *Prunus persica* seeds extract on carbon tetrachloride-induced hepatic injury in rats. *Chem. Pharm. Bull.* 23, 158–170. <https://doi.org/10.1217/1389201022666210203142138>.
- Rejiya, C.S., Cibin, T.R., Abraham, A., 2009. Leaves of *Cassia tora* as a novel cancer therapeutic – an in vitro study. *Toxicol. Vitro* 23, 1034–1038. <https://doi.org/10.1016/j.tiv.2009.06.010>.
- Reuland, D.J., Khademi, S., Castle, C.J., Irwin, D.C., McCord, J.M., Miller, B.F., Hamilton, K.L., 2013. Upregulation of phase II enzymes through phytochemical activation of Nrf2 protects cardiomyocytes against oxidant stress. *Free Radic. Biol. Med.* 56, 102–111. <https://doi.org/10.1016/j.freeradbiomed.2012.11.016>.
- Seo, J.Y., Pyo, E., An, J.-P., Kim, J., Sung, S.H., Oh, W.K., 2017. Andrographolide activates keap1/nrf2/ARE/HO-1 pathway in HT22 cells and suppresses microglial activation by  $\beta$  42 through nrf2-related inflammatory response. *Mediat. Inflamm.* 1–12. <https://doi.org/10.1155/2017/5906189>, 2017.
- Shang, L., Liu, Y., Li, J., Pan, G., Zhou, F., Yang, S., 2021. Emodin protects sepsis associated damage to the intestinal mucosal barrier through the VDR/Nrf2/HO-1 pathway. *Front. Pharmacol.* 12, 724511 <https://doi.org/10.3389/fphar.2021.724511>.
- Sharif-Rad, J., Herrera-Bravo, J., Kamiloglu, S., Petroni, K., Mishra, A.P., Monserrat-Mesquida, M., Sureda, A., Martorell, M., Aidarbekovna, D.S., Yessimsitova, Z., Ydyrys, A., Hano, C., Calina, D., Cho, W.C., 2022. Recent advances in the therapeutic potential of emodin for human health. *Biomed. Pharmacother.* 154, 113555 <https://doi.org/10.1016/j.biopha.2022.113555>.
- Shelton, L.M., Lister, A., Walsh, J., Jenkins, R.E., Wong, M.H.L., Rowe, C., Ricci, E., Ressel, L., Fang, Y., Demougin, P., Vukojevic, V., O'Neill, P.M., Goldring, C.E., Kitteringham, N.R., Park, B.K., Odermatt, A., Coppel, I.M., 2015. Integrated transcriptomic and proteomic analyses uncover regulatory roles of Nrf2 in the kidney. *Kidney Int.* 88, 1261–1273. <https://doi.org/10.1038/ki.2015.286>.
- Shen, C.-H., Liu, C.-T., Song, X.-J., Zeng, W.-Y., Lu, X.-Y., Zheng, Z.-L., Pan, Jie-, Zhan, R.-T., Ping, Yan, 2018. Evaluation of analgesic and anti-inflammatory activities of *Rubia cordifolia* L. by spectrum-effect relationships. *J. Chromatogr. B* 1090, 73–80. <https://doi.org/10.1016/j.jchromb.2018.05.021>.
- Shen, B., Feng, H., Cheng, J., Li, Z., Jin, M., Zhao, L., Wang, Q., Qin, H., Liu, G., 2020. Geniposide alleviates non-alcohol fatty liver disease via regulating Nrf2/AMPK/mTOR signalling pathways. *J. Cell Mol. Med.* 24, 5097–5108. <https://doi.org/10.1111/jcmm.15139>.
- Shen, P., Han, L., Chen, G., Cheng, Z., Liu, Q., 2022. Emodin attenuates acetaminophen-induced hepatotoxicity via the cGAS-STING pathway. *Inflammation* 45, 74–87. <https://doi.org/10.1007/s10753-021-01529-5>.
- Singh, J., Hussain, Y., Luqman, S., Meena, A., 2021. Purpurin: a natural anthraquinone with multifaceted pharmacological activities. *Phytother Res.* 35, 2418–2428. <https://doi.org/10.1002/ptr.6965>.
- Soib, H.H., Ismail, H.F., Husin, F., Abu Bakar, M.H., Yaakob, H., Sarmidi, M.R., 2020. Bioassay-guided different extraction techniques of *Carica papaya* (Linn.) leaves on in vitro wound-healing activities. *Molecules* 25, 1–13. <https://doi.org/10.3390/molecules25030517>.
- Su, S., Wu, J., Gao, Y., Luo, Y., Yang, D., Wang, P., 2020. The pharmacological properties of chrysophanol, the recent advances. *Biomed. Pharmacother.* 125, 110002 <https://doi.org/10.1016/j.biopha.2020.110002>.
- Tao, S., Justiniano, R., Zhang, D.D., Wondrak, G.T., 2013. The Nrf2-inducers tanshinone I and dihydrotanshinone protect human skin cells and reconstructed human skin against solar simulated UV. *Redox Biol.* 1, 532–541. <https://doi.org/10.1016/j.redox.2013.10.004>.
- Teschke, R., Wolff, A., Frenzel, C., Eickhoff, A., Schulze, J., 2015. Herbal traditional Chinese medicine and its evidence base in gastrointestinal disorders. *WJG* 21, 4466–4490. <https://doi.org/10.3748/wjg.v21.i15.4466>.
- Tessier, A.M., Delaveau, P., Champion, B., 1981. Nouvelles Anthraquinones des *Racines* de *Rubia cordifolia* 41, 337–343. <https://doi.org/10.1055/s-2007-971724>.
- Thorne, N., Auld, D.S., Inglese, J., 2010. Apparent activity in high-throughput screening: origins of compound-dependent assay interference. *Curr. Opin. Chem. Biol.* 14, 315–324. <https://doi.org/10.1016/j.cbpa.2010.03.020>.
- Tian, S.-L., Yang, Y., Liu, X.-L., Xu, Q.-B., 2018. Emodin attenuates bleomycin-induced pulmonary fibrosis via anti-inflammatory and anti-oxidative activities in rats. *Med. Sci. Mon. Int. Med. J. Exp. Clin. Res.* 24, 1–10. <https://doi.org/10.12659/MSM.905496>.
- van der Linden, S.C., von Bergh, A.R.M., van Vught-Lussenburg, B.M.A., Jonker, L.R.A., Teunis, M., Krul, C.A.M., van der Burg, B., 2014. Development of a panel of high-throughput reporter-gene assays to detect genotoxicity and oxidative stress. *Mutat.*

- Res. Genet. Toxicol. Environ. Mutagen 760, 23–32. <https://doi.org/10.1016/j.mrgentox.2013.09.009>.
- Wang, Mengmeng, Ke, Y., Li, Y., Shan, Z., Mi, W., Cao, Y., Feng, W., Zheng, X., 2021b. The nephroprotective effects and mechanisms of rehmapicrogenin include ROS inhibition via an oestrogen-like pathway both in vivo and in vitro. *Biomed. Pharmacother.* 138, 111305 <https://doi.org/10.1016/j.biopha.2021.111305>.
- Wang, A., Jiang, H., Liu, Y., Chen, J., Zhou, X., Zhao, C., Chen, X., Lin, M., 2020. Rhein induces liver cancer cells apoptosis via activating ROS-dependent JNK/Jun/caspase-3 signaling pathway. *J. Cancer* 11, 500–507. <https://doi.org/10.7150/jca.30381>.
- Wang, N., Li, D.-Y., Niu, H.-Y., Zhang, Y., He, P., Wang, J.-H., 2013. 2-Hydroxy-3-methylanthraquinone from *Hedyotis diffusa* Willd induces apoptosis in human leukemic U937 cells through modulation of MAPK pathways. *Arch. Pharm. Res. (Seoul)* 36, 752–758. <https://doi.org/10.1007/s12272-013-0096-4>.
- Wang, M., Wang, Q., Yang, Q., Yan, X., Feng, S., Wang, Z., 2019. Comparison of anthraquinones, iridoid glycosides and triterpenoids in *Morinda officinalis* and *Morinda citrifolia* using UPLC/Q-TOF-MS and multivariate statistical analysis. *Molecules* 25, 160. <https://doi.org/10.3390/molecules25010160>.
- Wang, Y., Li, B., Zhang, X., 2019. *Scutellaria barbata* D. Don (SBD) protects oxygen glucose deprivation/reperfusion-induced injuries of PC12 cells by up-regulating Nrf2. *Artif. Cell Nanomed. Biotechnol.* 47, 1797–1807. <https://doi.org/10.1080/21691401.2019.1610413>.
- Wang, Guangjun, Fu, Y., Li, J., Li, Y., Zhao, Q., Hu, A., Xu, C., Shao, D., Chen, W., 2021a. Aqueous extract of *Polygonatum sibiricum* ameliorates ethanol-induced mice liver injury via regulation of the Nrf2/ARE pathway. *J. Food Biochem.* 45 <https://doi.org/10.1111/jfbc.13537>.
- Wang, Miaomiao, Yang, W., Liu, X., Liu, Q., Zheng, H., Wang, X., Shen, T., Wang, S., Ren, D., 2021c. Two new compounds with Nrf2 inducing activity from *Glycyrrhiza uralensis*. *Nat. Prod. Res.* 35, 4357–4364. <https://doi.org/10.1080/14786419.2020.1715398>.
- Wei, S., Yao, W., Ji, W., Wei, J., Peng, S., 2013. Qualitative and quantitative analysis of anthraquinones in rhubarbs by high performance liquid chromatography with diode array detector and mass spectrometry. *Food Chem.* 141, 1710–1715. <https://doi.org/10.1016/j.foodchem.2013.04.074>.
- Wen, Y.-L., He, Z., Hou, D.-X., Qin, S., 2021. Crocetin exerts its anti-inflammatory property in LPS-induced RAW264.7 cells potentially via modulation on the crosstalk between MEK1/JNK/NF-κB/iNOS pathway and Nrf2/HO-1 pathway. *Oxid. Med. Cell. Longev.* 2021, 1–18. <https://doi.org/10.1155/2021/6631929>.
- Wondrak, G., Villeneuve, N.F., Lamore, S.D., Bause, A.S., Jiang, T., Zhang, D.D., 2010. The cinnamon-derived dietary factor cinnamic aldehyde activates the nrf2-dependent antioxidant response in human epithelial colon cells. *Molecules* 15, 3338–3355. <https://doi.org/10.3390/molecules15053338>.
- Wong, S.Y., Tan, M.G.K., Wong, P.T.H., Herr, D.R., Lai, M.K.P., 2016. Andrographolide induces Nrf2 and heme oxygenase 1 in astrocytes by activating p38 MAPK and ERK. *J. Neuroinflammation* 13, 251. <https://doi.org/10.1186/s12974-016-0723-3>.
- Wu, S., Yue, Y., Tian, H., Li, Z., Li, X., He, W., Ding, H., 2013. *Carthamus red* from *Carthamus tinctorius* L. exerts antioxidant and hepatoprotective effect against CCl4-induced liver damage in rats via the Nrf2 pathway. *J. Ethnopharmacol.* 148, 570–578. <https://doi.org/10.1016/j.jep.2013.04.054>.
- Yang, X., Chen, L., Liu, C., Qin, Y., Tang, Y., Li, S., 2017. Rapid screening, separation, and detection of α-glucosidase inhibitors from *Hedyotis diffusa* by ultrafiltration-liquid chromatography tandem mass spectrometry-high-speed countercurrent chromatography. *Med. Chem. Res.* 26, 3315–3322. <https://doi.org/10.1007/s00044-017-2024-5>.
- Yuan, K., Chen, S., Chen, X., Yao, S., Wang, X., Song, H., Zhu, M., 2020. High effective extraction of selected anthraquinones from *Polygonum multiflorum* using ionic liquids with ultrasonic assistance. *J. Mol. Liq.* 314, 113342 <https://doi.org/10.1016/j.molliq.2020.113342>.
- Zahn, M., Trinh, T., Jeong, M.L., Wang, D., Abeysinghe, P., Jia, Q., Ma, W., 2008. A reversed-phase high-performance liquid chromatographic method for the determination of aloesin, aloeresin a and anthraquinone in *Aloe ferox*: phytochem. *Anales* 19, 122–126. <https://doi.org/10.1002/pca.1024>.
- Zeng, G., An, H., Fang, D., Wang, W., Han, Y., Lian, C., 2022. Plantamajoside protects H9c2 cells against hypoxia/reoxygenation-induced injury through regulating the akt/Nrf2/HO-1 and NF-κB signaling pathways. *J. Recept. Signal Transduction* 42, 125–132. <https://doi.org/10.1080/10799893.2020.1859534>.
- Zhang, W., Wang, Y., Wang, Q., Yang, W., Gu, Y., Wang, R., Song, X., Wang, X., 2012. Quality evaluation of Semen Cassiae (*Cassia obtusifolia*L.) by using ultra-high performance liquid chromatography coupled with mass spectrometry: liquid Chromatography. *J. Sep. Science* 35, 2054–2062. <https://doi.org/10.1002/jssc.201200009>.
- Zhang, W.-J., Wang, S., Kang, C., Lv, C., Zhou, L., Huang, L.-Q., Guo, L.-P., 2020. Pharmacodynamic material basis of traditional Chinese medicine based on biomacromolecules: a review. *Plant Methods* 16, 26. <https://doi.org/10.1186/s13007-020-00571-y>.
- Zhang, K., Fang, K., Wang, T., Xu, L., Zhao, Y., Wang, X., Xiang, L., Shen, T., 2021. Chemical constituents from the rhizome of *Ligusticum chuanxiong* hort. And their Nrf2 inducing activity. *Chem. Biodiversity* 18. <https://doi.org/10.1002/cbdv.202100302>.
- Zhuang, S., Zhong, J., Bian, Y., Fan, Y., Chen, Q., Liu, P., Liu, Z., 2019a. Rhein ameliorates lipopolysaccharide-induced intestinal barrier injury via modulation of Nrf2 and MAPKs. *Life Sci.* 216, 168–175. <https://doi.org/10.1016/j.lfs.2018.11.048>.
- Zhuang, S., Zhong, J., Zhou, Q., Zhong, Y., Liu, P., Liu, Z., 2019b. Rhein protects against barrier disruption and inhibits inflammation in intestinal epithelial cells. *Int. Immunopharm.* 71, 321–327. <https://doi.org/10.1016/j.intimp.2019.03.030>.